EISSN: 2231-0916 doi: 10.14202/vetworld.2026.5011-5034 OPEN ACCESS

Veterinary World

RESEARCH ARTICLE

# BAJISAN extract improves semen quality and sperm motility in rabbits: a potential association with the PTEN/mTOR/Akt1/HSPA2 pathway

Shiyong Wang[1], Yao Chen[1,2,3], Yunhe Wang[1], Mingliang Luo[1], Jie Wu[2,3], Yuechun Yang[1], and Jing Zhang[1]

1. Institute of Laboratory Animal Science, Guizhou University of Traditional Chinese Medicine, Guiyang, Guizhou 550025, P. R. China.
2. College of Basic Medicine, Zunyi Medical University, Zunyi, Guizhou 563000, P. R. China.
3. Scientific Research Center, Third Affiliated Hospital of Zunyi Medical University (First People's Hospital of Zunyi), Zunyi, Guizhou 563000, P. R. China.

## ABSTRACT

**Background and Aim:** BAJISAN is a traditional Chinese herbal formula used for male reproductive disorders; however, its bioactive constituents and mechanisms underlying improvements in sperm function remain insufficiently characterized. This study aimed to investigate the dose-dependent effects of BAJISAN extract (BJSE) on semen quality, sperm motility, reproductive hormones, and testicular molecular signaling in rabbits through integrated chemical profiling, network pharmacology, and *in vivo* validation.

**Materials and Methods:** Twenty-four male New Zealand rabbits were randomly allocated to four groups (n = 6/group): control and BJSE treatment at 150, 300, or 600 mg/kg body weight daily for 16 weeks. Chemical constituents were characterized using ultra-high-performance liquid chromatography coupled with quadrupole-Orbitrap mass spectrometry. Network pharmacology, pathway enrichment, and molecular docking were performed to identify potential bioactive targets. Semen quality and sperm kinematics were evaluated longitudinally using computer-assisted sperm analysis. Serum reproductive hormones, testicular histology, and gene and protein expression were assessed to investigate treatment-associated reproductive and molecular changes.

**Results:** Chemical profiling identified 29 major constituents, including five compounds confirmed using reference standards. Network analysis highlighted steroid hormone-associated targets and phosphatidylinositol 3-kinase/protein kinase B signaling. BJSE significantly improved sperm survival, acrosome integrity, motility, and kinematic parameters while reducing sperm abnormalities, with the strongest responses generally observed at 600 mg/kg ($p < 0.05$). Significant dose-response trends were identified for major semen quality outcomes. Treatment increased serum luteinizing hormone, follicle-stimulating hormone, and testosterone concentrations during earlier reproductive development, although the direction and magnitude of these hormonal differences changed by week 16; significant between-group differences persisted for FSH, LH, and testosterone. Histological examination suggested improved seminiferous epithelial organization. Testicular analyses demonstrated reduced phosphatase and tensin homolog (PTEN) expression and increased mechanistic target of rapamycin (mTOR), AKT serine/threonine kinase 1 (Akt1), and heat shock protein family A member 2 (HSPA2) expression at both transcript and protein levels ($p < 0.05$).

**Conclusion:** BJSE improved semen quality and sperm motility in rabbits in association with coordinated changes in PTEN, mTOR, Akt1, and HSPA2 expression. These findings provide preclinical evidence supporting further investigation of BJSE for male reproductive dysfunction. However, pathway activation and causal mechanisms require confirmation through phosphorylation analyses and targeted functional experiments.

**Keywords:** BAJISAN extract, male reproductive health, network pharmacology, PTEN/mTOR/Akt1/HSPA2 pathway, rabbit semen quality, sperm motility, testicular function, traditional Chinese medicine.

## INTRODUCTION

Infertility is a major global reproductive health concern, affecting approximately 15% of couples worldwide [1, 2]. Reduced sperm motility is an important contributing factor to male infertility and is frequently observed in clinical reproductive assessments [3]. Sperm motility is not only a fundamental parameter of semen quality but

**Corresponding Author:** Yuechun Yang and Jing Zhang and JIng Zhang
**E-mail:** 54877887@qq.com; jingzhang666999@163.com

**Received:** 13-07-2026, **Accepted:** 12-10-2026, **Published online:** 09-11-2026

**Co-authors:** SW: shywang2004@126.com; YC: cy1008sanger@163.com; YW: 1134932397@qq.com; ML: 15085565499@163.com; JW: zhiwenwujie@163.com

**How to cite:** Wang S, Chen Y, Wang Y, Luo M, Wu J, Yang Y, *et al.* BAJISAN extract improves semen quality and sperm motility in rabbits: a potential association with the PTEN/mTOR/Akt1/HSPA2 pathway. Vet World. 2026;19(11):5011–5034.

**Copyright:** Wang *et al*. This article is an open access article distributed under the terms of the Creative Commons Attribution 4.0 International License (https://creativecommons.org/licenses/by/4.0/).

also essential for successful fertilization, enabling spermatozoa to traverse the female reproductive tract and penetrate the oocyte [4, 5]. Conventional interventions, including hormonal therapies and antioxidant supplementation, have demonstrated variable therapeutic outcomes and may be associated with adverse effects, highlighting the need to investigate alternative approaches for improving male reproductive function [6–12].

Traditional Chinese medicine (TCM) has attracted increasing scientific interest because of its multicomponent and multitarget approaches to managing reproductive dysfunction [13–19]. BAJISAN is a classical TCM formulation first documented in the *Taiping Shenghui Fang* (*Taiping Holy Prescriptions for Universal Relief*) during the Song Dynasty in 992 AD [20]. Traditionally, practitioners have used the formulation to address infertility-related conditions based on the TCM principle of "warming the kidney and activating yang."

BAJISAN comprises 11 herbal ingredients: Ba Ji Tian (*Morinda officinalis*), Rou Cong Rong (*Cistanche deserticola*), Bu Gu Zhi (*Psoralea corylifolia*), Hui Xiang (*Foeniculum vulgare*), Rou Gui Pi (*Cinnamomum cassia*), Chenpi Gan (*Citri Reticulatae Pericarpium*, dried tangerine peel), Qingju Pi (*Citri Reticulatae Pericarpium Viride*, green tangerine peel), Rou Dou Kou (*Myristica fragrans*), Du Zhong (*Eucommia ulmoides*), Ku Jian Pi (*Melia toosendan* fruit), and Bing Lang Guo (*Areca catechu*). Researchers have investigated several constituents of this formulation for their potential reproductive and pharmacological activities. In particular, *C. deserticola* [21, 22], *P. corylifolia* [23], and *F. vulgare* [24] have been associated with traditional applications involving reproductive function, including the regulation of kidney essence, circulation, and endometrial development [25]. Experimental investigations have also demonstrated that *F. vulgare* essential oil can upregulate estrogen receptor 2 (ESR2) expression in laying hens [26]. However, the pharmacological activities of individual herbal constituents do not necessarily establish the biological effects or mechanisms of the complete BAJISAN formulation.

Network pharmacology provides a systematic approach for investigating the potential mechanisms of multicomponent herbal formulations by identifying interactions among bioactive compounds, molecular targets, and biological pathways [27, 28]. Advances in reproductive biology have identified several signaling pathways involved in spermatogenesis, sperm maturation, and cellular homeostasis. Among these, the phosphatidylinositol 3-kinase (PI3K)/protein kinase B (Akt)/mechanistic target of rapamycin (mTOR) signaling pathway plays an important role in regulating cellular proliferation, survival, metabolism, and spermatogenic function. Phosphatase and tensin homolog (PTEN) acts as a negative regulator of PI3K/Akt signaling [29–34].

Several proteins involved in reproductive regulation, including androgen receptor (AR), aurora kinase A (AURKA), estrogen receptor 1 (ESR1), and SRC proto-oncogene, non-receptor tyrosine kinase (SRC), have functional associations with signaling networks relevant to male fertility [35–44]. In addition, heat shock protein family A member 2 (HSPA2), a molecular chaperone involved in germ cell development and sperm maturation, contributes to the maintenance of sperm function and motility [45, 46]. These molecular interactions provide a biological framework for investigating whether BAJISAN extract (BJSE) influences sperm quality through coordinated changes in reproductive signaling pathways.

Despite the traditional application of BAJISAN in managing male reproductive disorders, its chemical composition, potential molecular targets, and effects on sperm function have not been comprehensively characterized using an integrated experimental approach. Previous investigations of TCM formulations for male infertility have frequently relied on computational predictions or assessments of individual herbal constituents, without systematically linking chemical composition to predicted molecular interactions and experimentally measured reproductive outcomes [16, 26]. Consequently, the relationship between BAJISAN's bioactive constituents and their potential effects on semen quality, sperm motility, reproductive hormones, and testicular function remains poorly understood.

Furthermore, although the PI3K/Akt/mTOR signaling pathway and HSPA2 are involved in reproductive cellular processes, their potential association with BAJISAN-mediated changes in sperm function has not been adequately investigated. In particular, evidence linking computationally predicted upstream targets, including AR, AURKA, ESR1, and SRC, with experimentally measured changes in PTEN, mTOR, Akt1, and HSPA2 expression following BAJISAN administration remains limited. Existing evidence also does not adequately establish whether BAJISAN produces dose-dependent improvements in semen quality during prolonged administration or whether such improvements are accompanied by consistent hormonal, histological, and molecular changes.

Addressing these gaps requires an integrated strategy combining high-resolution chemical profiling, network pharmacology, molecular docking, and longitudinal *in vivo* evaluation. Such an approach can distinguish predicted compound–target interactions from experimentally observed biological responses and provide a more comprehensive understanding of the potential mechanisms associated with BAJISAN administration. Importantly,

changes in gene and protein expression must be distinguished from direct evidence of pathway activation or causal molecular regulation.

This study aimed to investigate the effects of BJSE on semen quality, sperm motility, reproductive hormone concentrations, and testicular function in male rabbits and to explore the molecular mechanisms potentially associated with these effects. Specifically, the study sought to characterize the major chemical constituents of BJSE using ultra-high-performance liquid chromatography coupled with quadrupole-Orbitrap mass spectrometry (UPLC-Q-Orbitrap MS), identify potential bioactive targets through network pharmacology, and evaluate predicted compound–target interactions using molecular docking.

The study further aimed to assess the dose-dependent effects of daily BJSE administration at 150, 300, and 600 mg/kg body weight over 16 weeks on sperm motility, kinematic parameters, sperm survival, acrosome integrity, and morphological abnormalities. The study evaluated serum reproductive hormone concentrations and testicular histological characteristics to investigate treatment-associated changes in reproductive function.

At the molecular level, the study examined PTEN, mTOR, AKT serine/threonine kinase 1 (Akt1), and HSPA2 expression in testicular tissue to determine whether improvements in semen quality were associated with coordinated changes in these signaling-related proteins. The central hypothesis was that BJSE administration would improve sperm quality and motility in a dose-dependent manner, accompanied by changes in the PTEN/mTOR/Akt1/HSPA2 signaling-related axis. By integrating computational predictions with *in vivo* observations, the study sought to provide preclinical evidence for the potential reproductive effects of BJSE and establish a foundation for further mechanistic and functional validation.

## MATERIALS AND METHODS

### Ethical approval

The experimental protocol was reviewed and approved by the Ethics Committee of the Institute of Laboratory Animals, Guizhou University of Chinese Medicine, China (approval number: 20240430001, dated 30-04-2024). All rabbit procedures were performed in accordance with the National Standard for Guidelines for Ethical Review of Laboratory Animal Welfare (GB/T 35892-2018). Rabbits were housed under controlled environmental conditions and monitored daily for signs of illness, abnormal behavior, or changes in appetite. Animals exhibiting illness, abnormal appetite, or failure to demonstrate mounting behavior were designated for exclusion; however, none met these criteria during the study. Animal use was minimized while maintaining the experimental design necessary to evaluate reproductive outcomes. At the end of the study, rabbits were euthanized by National Standard for Euthanasia of Laboratory Animals (GB/T 39760-2021), and death was confirmed before tissue collection.

### Study period and location

The experimental procedures were conducted at the Institute of Zoology, Guizhou University of Traditional Chinese Medicine (TCM), China, between June 2024 and October 2024. The animal experiment lasted 16 weeks, preceded by a 1-week acclimatization period. Semen quality was evaluated at weeks 10, 12, 14, and 16, whereas blood samples were collected for hormonal assessment at weeks 8, 10, and 16.

### Study design

This experimental study integrated chemical profiling, network pharmacology, molecular docking, and *in vivo* validation to investigate the effects of BJSE on male reproductive function. Twenty-four 7-month-old male New Zealand rabbits were randomly assigned to four groups (n = 6/group): control, low-dose BJSE (BJSE-L; 150 mg/kg body weight), medium-dose BJSE (BJSE-M; 300 mg/kg), and high-dose BJSE (BJSE-H; 600 mg/kg). Treatments were administered daily by oral gavage for 16 weeks.

The primary outcomes were sperm survival and motility parameters, whereas reproductive hormone concentrations, testicular histology, and gene and protein expression were evaluated as secondary or exploratory outcomes. The study also investigated dose-response relationships and potential associations between reproductive changes and expression of signaling-related proteins.

### Chemical composition analysis of BJSE

BAJISAN consisted of 11 herbal ingredients: 45 g of *Morinda officinalis*, 45 g of *Cistanche deserticola*, 45 g of *Psoralea corylifolia*, 45 g of *Foeniculum vulgare*, 30 g of *Cinnamomum cassia*, 30 g of dried tangerine peel, 30 g of green tangerine peel, 30 g of *Myristica fragrans*, 20 g of *Eucommia ulmoides*, 20 g of *Melia toosendan* fruit, and

15 g of *Areca catechu*. All herbal materials were purchased from Hubei Jiulingcao Biotechnology Co., Ltd. (Wuhan, Hubei, China).

The dried herbal materials were ground into powder and extracted with water at a material-to-solvent ratio of 1:15 (w/v), following the traditional decoction method used for BAJISAN. The mixture was boiled for 2 h and filtered to collect the aqueous extract. The extraction procedure was repeated twice, and the three filtrates were combined. The combined extract was centrifuged at 3000 × *g* for 15 min to remove suspended particles.

The resulting supernatant was concentrated on a rotary evaporator under reduced pressure (0.08 MPa) at 60°C until it reached a relative density of 1.06 at 20°C. The concentrated extract was then spray-dried at an inlet temperature of 160–180°C, an outlet temperature of 80–90°C, and an atomization pressure of 0.2–0.3 MPa. The resulting brown powder was designated BJSE and stored for subsequent experiments. The extraction yield was approximately 18.2% (w/w). The same batch of BJSE was used throughout the study.

For chemical analysis, 0.1 g of BJSE was mixed with 1 mL of 80% methanol and grinding beads. The mixture was ground for 5 min, vortexed for 10 min, and centrifuged at 20,000 × *g* for 10 min at 4°C. The supernatant was analyzed using a Q Exactive high-resolution mass spectrometer (Thermo Fisher Scientific, China) operated in full-scan MS/data-dependent tandem MS (Full MS/dd-$MS^2$) mode, with resolutions of 70,000 and 17,500, respectively.

Data were acquired during a 30-min analytical run using an electrospray ionization source operated in positive- and negative-ion switching modes, with a spray voltage of 3.2 kV and a mass-to-charge ratio (m/z) scanning range of 100.0–1500.0. Chromatographic separation was performed using an AQ–C18 column (150 × 2.1 mm, 1.8 µm; Welch) maintained at 35°C, with a mobile-phase flow rate of 0.30 mL/min. The mobile phases consisted of 0.1% formic acid in water and methanol.

Data acquisition was performed using Chromeleon software, version 7.3 (Thermo Fisher Scientific). Compounds were identified by matching accurate-mass precursor-ion and fragmentation spectra against the mzCloud database.

Compound identification confidence was classified according to the Metabolomics Standards Initiative guidelines. Level 1 identification was assigned to compounds confirmed by comparing retention times and tandem MS fragmentation patterns with authentic reference standards analyzed by the commercial service provider under identical LC–MS conditions. The matching was performed against the provider's in-house standard library. Level 2 identification was assigned to compounds tentatively identified through high-resolution spectral matching against mzCloud (match score >80), supported by consistency with previously reported constituents of the component herbs.

Five compounds were confirmed at Level 1: baicalin (compound 2), hesperidin (compound 11), orientin (compound 13), vitexin (compound 26), and naringin (compound 28). These compounds are indicated by asterisks in Figure 1B. The remaining compounds presented in Figure 1 were tentatively identified at Level 2.

**Bioactive component identification and network pharmacology analysis**

Identification of potential targets: The chemical constituents of BJSE were characterized through untargeted qualitative profiling using ultra-high-performance liquid chromatography coupled with quadrupole-Orbitrap MS (UPLC-Q-Orbitrap MS, Servicebio, Wuhan, China). Because the analysis was qualitative rather than quantitative, formal validation parameters, including linearity, limit of detection, and limit of quantification, were not determined.

Canonical simplified molecular input line entry system (SMILES) representations of the identified compounds were retrieved from PubChem (https://pubchem.ncbi.nlm.nih.gov/; accessed January 2025). Physicochemical properties, pharmacokinetics, and drug-likeness were evaluated using SwissADME (http://www.swissadme.ch/; accessed January 2025) with default parameters; compounds were retained for target prediction if they complied with the Lipinski rule-of-five with zero violations and an Abbott bioavailability score > 0.55. Compound-associated protein targets were then predicted using SwissTargetPrediction (http://www.swisstargetprediction.ch/; accessed January 2025), with the organism restricted to Homo sapiens and a probability threshold > 0.1. Potential targets associated with male reproductive function were retrieved from GeneCards (https://www.genecards.org/; accessed January 2025) using the keywords "sperm motility," "Leydig cell," and "spermatogenesis," with the organism restricted to *Homo sapiens*. Human databases were selected because of their extensive functional annotations and the reported conservation of the PI3K/Akt/mTOR signaling pathway among mammals.

A GeneCards relevance score >5 was used to retain potentially relevant targets. This threshold was selected

according to the laboratory's established analytical approach. Sensitivity analyses using alternative relevance thresholds were not performed.

Predicted compound-associated targets and reproductive function-associated targets were standardized to official gene symbols using UniProt (https://www.uniprot.org/; accessed January 2025). Overlapping targets were identified using an online Venn diagram tool (http://www.bioinformatics.com.cn; accessed January 2025). To improve specificity, only targets identified in at least two of the three reproductive keyword searches were retained.

The resulting overlapping targets were considered candidate molecular targets potentially associated with the reproductive effects of BJSE. Although several targets and signaling components are conserved across mammals, formal ortholog mapping and sequence identity calculations between human and rabbit proteins were not performed.

Protein–protein interaction (PPI) network construction: The overlapping genes were uploaded to the STRING database (version 11.5; https://cn.string-db.org/; accessed January 2025) to construct a PPI network [47]. A minimum interaction confidence score of 0.400 was applied. Evidence from experiments, curated databases, co-expression, text mining, and homology was included, and disconnected nodes were excluded from network visualization.

The PPI network was visualized using Cytoscape software, version 3.10.1 (https://so915.dltmer.cn/s/cytoscape-bioinformatics-tool/). Network topology was evaluated using degree, betweenness centrality, and closeness centrality. Hub genes were identified using the CytoHubba plugin and ranked according to the maximal clique centrality algorithm, with the 10 highest-ranked genes selected.

Functional modules were identified using the Molecular Complex Detection (MCODE) plugin with the following parameters: degree cutoff = 2, node score cutoff = 0.2, K-core = 2, and maximum depth = 100.

Functional enrichment of the identified modules was performed using the STRING enrichment tool (https://cn.string-db.org/). The results were visualized using the ggplot2 package in R software, version 4.2.0 (http://had.co.nz/ggplot2/), with gene annotation support from the Hs.eg.db database (https://bioconductor.org/packages/release/data/annotation/html/org.Hs.eg.db.html).

Functional and pathway enrichment analysis: Gene Ontology (GO) and Kyoto Encyclopedia of Genes and Genomes (KEGG) pathway enrichment analyses were performed using the identified candidate targets. GO enrichment included biological process, molecular function, and cellular component categories.

Statistical significance was determined using the Benjamini–Hochberg false discovery rate-adjusted p-value, with $p \leq 0.01$ considered significant. The 20 most significantly enriched KEGG pathways were selected and categorized according to the KEGG PATHWAY database.

A target–pathway interaction network was constructed using Cytoscape. Node size and color intensity were proportional to node degree.

**Molecular docking analysis**

Molecular docking was performed to predict interactions between the identified BJSE constituents and selected target proteins, following previously described procedures [48].

Three-dimensional protein structures were obtained from the Protein Data Bank (PDB; https://www.rcsb.org/; accessed January 2025). The selected structures were AR (PDB ID: 5XPN), AURKA (5DPV), ESR1 (4XI3), nuclear receptor subfamily 3 group C member 1 (NR3C1; 3E7C and 4NH5), and SRC (5JMM).

The three-dimensional structures of the selected compounds were obtained from the Traditional Chinese Medicine Systems Pharmacology database (https://tcmsp-e.com/; accessed January 2025).

Ligand structures were prepared using Open Babel, version 3.1.1 (https://github.com/openbabel), to generate three-dimensional conformations, assign Gasteiger charges, and define rotatable bonds. Protein structures were prepared using AutoDock Tools, version 1.5.7 (https://github.com/ccsb-scripps) by adding hydrogen atoms, assigning Kollman charges, merging nonpolar hydrogen atoms, and saving the structures in PDBQT format [49]. Crystallographic water molecules were removed, except for conserved structural waters considered essential for protein stability.

Docking simulations were conducted using AutoDock Vina, version 1.2.3, with an exhaustiveness value of 8, a maximum of 20 docking poses per ligand, and an energy range of 3 kcal/mol for pose clustering [50]. Grid-box coordinates and dimensions for individual target proteins are provided in Supplementary Table S1.

The final docking pose was selected as the lowest-energy conformation within the highest-ranked cluster,

using a root-mean-square deviation (RMSD) threshold <2.0 Å from the cluster centroid. Predicted binding affinities were visualized using the pheatmap package in R. Interactions with predicted binding energies <−7.0 kcal/mol were further examined using PyMOL, version 2.5.0 (https://www.pymol.org/).

**Molecular docking protocol validation**

The docking protocol was evaluated by re-docking the native ligand of each selected protein complex. The co-crystallized ligand was extracted and re-docked into the prepared protein structure using the same parameters applied to the BJSE compounds.

The RMSD between the heavy atoms of the re-docked ligand and its original crystallographic conformation was calculated using PyMOL. The resulting RMSD values were 1.25 Å for AR, 1.78 Å for AURKA, 0.95 Å for ESR1, 1.52 Å for NR3C1, and 1.41 Å for SRC.

All RMSD values were below 2.0 Å, indicating that the docking procedure reproduced the reference ligand-binding orientations within the predefined validation threshold. These results supported the suitability of the docking protocol for comparative prediction of compound–target interactions.

**Experimental animals, housing, and treatment allocation**

Twenty-four healthy, 7-month-old male New Zealand rabbits, with a mean body weight of 2.75 ± 0.50 kg, were obtained from the Institute of Zoology, Guizhou University of TCM.

The rabbits were housed individually in stainless steel cages measuring 60 × 50 × 40 cm under controlled environmental conditions of 20–22°C, 50%–60% relative humidity, and a 12-h light/12-h dark cycle. A commercial rabbit pellet diet containing 18% protein, 4% fat, and 14% fiber was provided, with drinking water available *ad libitum*.

After a 1-week acclimatization period, the rabbits were randomly allocated to four experimental groups using a computer-generated randomization list. Each group contained six animals.

The control group received distilled water at 2 mL/kg body weight by oral gavage. The BJSE-L, BJSE-M, and BJSE-H groups received BJSE at 150, 300, and 600 mg/kg body weight/day, respectively, dissolved in distilled water at an administration volume of 2 mL/kg body weight.

The selected doses corresponded to approximately 0.5, 1, and 2 times the calculated human-equivalent dose derived from the traditional clinical formulation. Treatment doses were adjusted weekly according to individual body weights. All treatments were administered daily for 16 weeks.

Personnel responsible for preparing and administering treatments were aware of group allocation. However, semen collection and analysis, hormone assays, histological examinations, and molecular analyses were performed by researchers blinded to the experimental groups.

The sample size of six rabbits per group was selected based on published rabbit reproductive studies commonly involving 5–8 animals per group and the principle of minimizing animal use. A post hoc power analysis using observed effect sizes (Cohen's d = 0.86–7.80 for key outcomes) indicated statistical power >80% for the observed differences. No formal *a priori* sample-size calculation was performed.

**Behavioral conditioning for semen collection**

A behavioral conditioning protocol based on olfactory stimulation was used to facilitate semen collection with an artificial vagina [51].

Following acclimatization, two or three similarly colored artificial rabbit pelts were placed in each cage. During routine cage cleaning, the pelts were transferred to female rabbit cages for 5 min to acquire female-associated odors.

The scented pelts were subsequently draped over the experimenter's right forearm to stimulate mounting behavior in the male rabbits. Mounting responses were recorded, and the conditioning procedure was repeated over 2–3 weeks to familiarize the animals with the collection procedure.

**Determination of serum reproductive hormone concentrations**

Blood samples were collected at weeks 8, 10, and 16. Week 10 samples were not used for hormone quantification; hormonal statistical analysis therefore included only weeks 8 and 16.

Serum concentrations of follicle-stimulating hormone (FSH), luteinizing hormone (LH), and testosterone were measured using commercial enzyme-linked immunosorbent assay (ELISA) kits (Jiancheng Bioengineering Institute, Nanjing, Jiangsu, China), following the manufacturer's instructions.

The FSH assay (catalog number H101-1-2) had a detection range of 1.56–100 mIU/mL and a sensitivity of

0.39 mIU/mL. The LH assay (catalog number H206-1-2) had a detection range of 0.156–100 mIU/mL and a sensitivity of 0.39 mIU/mL. The testosterone assay (catalog number H090-1-2) had a detection range of 0.5–50 ng/mL and a sensitivity of 0.1 ng/mL.

The reported intra-assay coefficients of variation were <8%, whereas the inter-assay coefficients of variation were <12%.

Hormone concentrations were expressed as absolute values. Comparisons were performed between BJSE-treated groups and the concurrently maintained control group, which served as the internal reference for evaluating treatment-associated hormonal changes.

**Semen collection and quality assessment**

Semen samples were collected at weeks 10, 12, 14, and 16 using an artificial vagina. Before collection, the artificial vagina and collection cup were cleaned, dried, and prewarmed in a water bath to 38–40°C. The artificial vagina was lubricated with saline, checked for patency, and connected to the collection cup.

The experimenter placed a female-scented artificial rabbit pelt over the forearm to stimulate mounting behavior. The experimenter collected semen immediately after the rabbit mounted the prepared collection apparatus.

At each scheduled collection, all six rabbits in every experimental group produced analyzable ejaculates. No semen samples were missing from the longitudinal dataset.

**Computer-assisted sperm analysis (CASA)**

Semen analysis was performed within 15 min of collection. The sperm counting chamber was prewarmed to 38°C.

A 10-µL aliquot of fresh semen was diluted with 90 µL of prewarmed modified Tris-citrate-fructose-egg yolk (TCFY) buffer. The diluent contained 2.4 g Tris (MedChemExpress, Shanghai, China) 1.4 g citric acid (MedChemExpress), 1.0 g fructose (MedChemExpress), 20 mL egg yolk (MedChemExpress), 0.1 g penicillin–streptomycin (MedChemExpress), and nuclease-free water (MedChemExpress) to a final volume of 100 mL. The pH was adjusted to 7.2. Subsequently, 10 µL of diluted semen was loaded into the counting chamber.

Sperm motility and kinematic parameters were assessed using a CASA system (TOX IVOS II, Shanghai, China) at 60 frames/s. The minimum sperm particle area was set at 4 µm², and the minimum detectable sperm velocity was 5 µm/s.

The evaluated kinematic parameters included average path velocity (VAP), curvilinear velocity (VCL), straight-line velocity (VSL), mean angular displacement (MAD), amplitude of lateral head displacement (ALH), and beat-cross frequency (BCF).

Spermatozoa were classified according to the following velocity criteria:

- Progressive motility: VAP ≥25 µm/s.
- Nonprogressive motility: VAP 5–25 µm/s.
- Immotility: VAP <5 µm/s.
- Grade A (rapid progressive): VAP ≥25 µm/s and VSL ≥20 µm/s.
- Grade B (slow progressive): VAP ≥25 µm/s and VSL <20 µm/s.
- Grade C (nonprogressive): VAP 5–25 µm/s.
- Grade D (immotile): VAP <5 µm/s.

Each semen sample was analyzed in triplicate, and the mean values were used for statistical evaluation.

In this study, sperm survival was operationally defined as the proportion of motile spermatozoa (VAP ≥ 5 µm/s) among total spermatozoa, as output by CASA. We acknowledge that this is a motility-based index rather than a membrane-integrity viability assay.

**Assessment of acrosome integrity and sperm abnormalities**

Thin semen smears were prepared by placing a small drop of semen approximately 1 cm from the end of a clean glass slide and spreading it into a uniform film.

The smears were air-dried for 10 min, fixed in 4% formaldehyde for 10 min, rinsed with distilled water, and air-dried again. The fixed smears were stained with Wright–Giemsa stain for 10 min, gently rinsed, and dried.

Stained spermatozoa were examined under a light microscope (ML-608SJ, Mailang Medical, Nanning, China) at 400× magnification. Acrosome integrity and sperm morphological abnormalities were assessed by examining 200 spermatozoa across five microscopic fields per slide.

Three replicate assessments were performed for each sample, and the mean values were used for statistical analysis.

**Collection and analysis of testicular tissue samples**

At the end of the 16-week experimental period, a final blood sample was collected before euthanasia. The testes were subsequently harvested for histological and molecular analyses.

A portion of each testis was fixed in 4% paraformaldehyde for histological examination, whereas the remaining tissue was snap-frozen and stored at −80°C until RNA and protein analyses.

**Histological examination**

Testicular tissue samples were fixed in 4% paraformaldehyde for 24 h, dehydrated through graded ethanol solutions (70%–100%), cleared in xylene, and embedded in paraffin. Serial sections measuring 4 μm in thickness were prepared using a microtome and stained with hematoxylin and eosin.

Histological sections were examined under a light microscope (ML-608SJ, Mailang Medical, Nanning, China) by two independent observers blinded to experimental group allocation.

The qualitative evaluation focused on seminiferous tubule architecture; the presence and organization of spermatogenic cells (spermatogonia, spermatocytes, and spermatids); and the appearance of the interstitial tissue.

The assessments aimed to identify morphological differences associated with spermatogenic activity rather than provide quantitative stereological measurements. Observers reported concordant assessments for all samples, and they resolved any discrepancies through discussion.

**RNA extraction and quantitative real-time polymerase chain reaction (qPCR)**

Total RNA was extracted from testicular tissues using the chloroform extraction method. RNA purity was assessed using absorbance ratios at 260/280 nm (acceptable range: 1.8–2.0) and 260/230 nm (>2.0). RNA integrity was evaluated by agarose gel electrophoresis.

Complementary DNA (cDNA) was synthesized using 1 μg of total RNA in a 20-μL reverse-transcription reaction containing PrimeScript RT Master Mix (Takara, Dalian, China), following the manufacturer's protocol.

qPCR was performed using a 20-μL reaction mixture containing 10 μL of 2× Universal Blue SYBR Green qPCR Master Mix (Takara), 0.4 μL each of forward and reverse primers (10 μM), 2 μL of diluted cDNA template (1:5), and RNase-free water.

Amplification efficiencies were evaluated using standard curves and ranged from 90% to 110%. The amplification protocol consisted of an initial denaturation at 95°C for 10 min, followed by 40 cycles of denaturation at 95°C for 25 s and annealing/extension at 60°C for 25 s. Melting-curve analysis was performed after amplification to confirm product specificity.

Relative gene expression was calculated using the 2^−ΔΔCt method, with glyceraldehyde-3-phosphate dehydrogenase (GAPDH) as the reference gene.

Primers were designed using Primer 5.0 software and synthesized by Sangon Biotechnology Co., Ltd. (Shanghai, China). The primer sequences and expected amplification product sizes are presented in Table 1.

**Table 1:** Primer sequences and expected amplification product sizes used for qPCR analysis of rabbit testicular gene expression.

| Gene | Primer | Sequence (5′–3′) | Product size (bp) |
|---|---|---|---|
| *mTOR* | Forward | CCCTTACCTCACAGGACATCG | 174 |
| | Reverse | GCTCCTTGTAGTGCAGGGCTTT | |
| *PTEN* | Forward | CACCGCCAAATTTAACTGCAGAG | 220 |
| | Reverse | TAGCGCCTCTGACTGGGAATAG | |
| *HSPA2* | Forward | AGATCATCGCCAACGACCAG | 117 |
| | Reverse | CCAGTGCTTCATGTCCGACT | |
| *GAPDH* | Forward | TGAAGGTCGGAGTGAACGGAT | 183 |
| | Reverse | CGTTCTCAGCCTTGACCGTG | |
| *AKT1* | Forward | AGTACATCAAGACCTGGCGG | 114 |
| | Reverse | AGTTGTTGAGTGGGGACTCG | |

bp = Base pairs; qPCR = Quantitative real-time polymerase chain reaction; *mTOR* = Mechanistic target of rapamycin; *PTEN* = Phosphatase and tensin homolog; *HSPA2* = Heat shock protein family A member 2; *GAPDH* = Glyceraldehyde-3-phosphate dehydrogenase; *AKT1* = AKT serine/threonine kinase 1. Forward and reverse primer sequences are presented in the 5′–3′ direction. Gene symbols are italicized.

The stability of *GAPDH* expression across experimental groups was assessed by comparing cycle threshold values. No statistically significant between-group differences were detected (one-way analysis of variance (ANOVA), $p > 0.05$). However, formal reference-gene stability testing using geNorm, NormFinder, or multiple candidate reference genes was not performed.

**Protein extraction and Western blot analysis**

Approximately 100 mg of testicular tissue was homogenized in 1 mL of radioimmunoprecipitation assay (RIPA) lysis buffer and incubated on ice for 10 min. The tissue homogenate was further processed using a precooled tissue grinder at −40°C and centrifuged at 12,000 × *g* for 15 min at 4°C.

The supernatant was collected, and total protein concentration was determined using a BCA protein assay kit (Beyotime, Shanghai, China), with bovine serum albumin (BSA) as the standard. Protein loading buffer was added, and the samples were heated for 10 min to denature the proteins.

For Western blot analysis, 40 μg of total protein was loaded per lane. Proteins were separated using 10% sodium dodecyl sulfate–polyacrylamide gel electrophoresis (SDS-PAGE) for PTEN, mTOR, Akt1, and β-actin and 12% SDS-PAGE for HSPA2.

Separated proteins were transferred to 0.45-μm polyvinylidene difluoride (PVDF) membranes (Millipore) using a wet transfer system at a constant voltage of 100 V for 90 min at 4°C. The membranes were blocked with 5% nonfat milk in Tris-buffered saline containing Tween 20 (TBST) for 1 h at 24°C.

Membranes were incubated overnight at 4°C with the following primary antibodies: rabbit monoclonal anti-PTEN (Abcam, shanghai, China, ab267787; 1:1000), rabbit monoclonal anti-mTOR (Abcam, ab32028; 1:2000), rabbit monoclonal anti-Akt1 (Abcam, ab179463; 1:1000), rabbit polyclonal anti-HSPA2 (Abcam, ab135828; 1:1000), and rabbit monoclonal anti-β-actin (Abcam, ab8227; 1:5000). Each target protein was analyzed on an independent membrane, with β-actin detected on the same membrane after stripping using a mild stripping buffer (Beyotime, Shanghai, China). Following washing, membranes were incubated with horseradish peroxidase-conjugated anti-rabbit secondary antibody (Abcam, ab6721; 1:5000) for 1 h at room temperature.

Protein bands were detected using Clarity Western enhanced chemiluminescence substrate (Bio-Rad China, https://www.bio-rad-china.com), with exposure times ranging from 30 s to 5 min. Bio-Rad Precision Plus protein markers were included for molecular-weight verification.

Band intensities were quantified using Image Lab software. Relative protein expression was normalized to β-actin. Antibody specificity was based on the manufacturer's reported rabbit reactivity for each antibody used. In-house knockdown or peptide-blocking validation in rabbit testicular tissue was not performed; this is acknowledged as a limitation. All six rabbits per group were included as independent biological replicates.

**Statistical analysis**

Data were compiled using Microsoft Excel and analyzed using SPSS software, version 27.0.1 (SPSS Inc., Chicago, IL, USA). Data normality and homogeneity of variance were evaluated using the Shapiro–Wilk and Levene tests, respectively. Results are expressed as mean ± standard error of the mean.

For semen quality parameters measured at weeks 10, 12, 14, and 16, a two-way repeated-measures ANOVA was performed. Treatment group (control, BJSE-L, BJSE-M, and BJSE-H) was included as the between-subjects factor and sampling time was included as the within-subjects factor. Repeated observations from the same rabbit were handled through the within-subject repeated-measures design.

Sphericity was assessed using Mauchly's test, and the Greenhouse–Geisser correction was applied when the sphericity assumption was violated. When a significant treatment × time interaction was detected, simple effects analysis was performed: between-group differences were evaluated at each time point using one-way ANOVA followed by Tukey's post hoc test, and within-group changes across time were evaluated using repeated-measures ANOVA followed by Tukey's test.

For endpoints measured at a single time point, differences among treatment groups were evaluated using one-way ANOVA followed by Tukey's post hoc test.

Hormonal data obtained at weeks 8 and 16 were analyzed using two-way repeated-measures ANOVA, with treatment group as the between-subjects factor and sampling time as the within-subjects factor. Treatment × time interactions were evaluated to determine whether hormonal responses differed across the experimental period.

Linear dose-response trends were assessed using simple linear regression at each sampling time point

separately, with administered BJSE dose (0, 150, 300, and 600 mg/kg body weight) as a continuous predictor. Because each rabbit contributed one observation per time point, repeated observations were not modeled jointly in this analysis. Linear trend analyses were performed for key outcome variables. Nonlinear dose-response relationships were not formally evaluated.

The primary outcomes were sperm survival rate and sperm motility parameters, including VAP, VCL, and VSL. Hormonal, histological, gene-expression, and protein-expression measurements were considered secondary or exploratory endpoints.

Cohen's d was calculated as the difference between group means divided by the pooled standard deviation, where $SD_pooled = \sqrt{[(SD_1^2 + SD_2^2)/2]}$ for equal group sizes (n = 6 per group). Standard deviations were derived from the reported standard errors of the mean ($SD = SEM \times \sqrt{n}$). Ninety-five percent confidence intervals for d were computed using the noncentral t distribution (two-tailed, $df = n_1 + n_2 - 2$).

Statistical significance was established at $p < 0.05$. No formal adjustment for multiple testing across all secondary outcomes was performed. Accordingly, findings from exploratory endpoints were interpreted with consideration of the potential for false-positive results.

## RESULTS

### Identification of chemical constituents in BJSE

Ultra-high-performance liquid chromatography coupled with quadrupole-Orbitrap MS (UPLC-Q-Orbitrap MS), performed in positive- and negative-ion modes, identified 29 major chemical constituents in BJSE (Figure 1).

The identified compounds were classified into two confidence levels. Five compounds were confirmed using authentic reference standards (Level 1): baicalin (compound 2), hesperidin (compound 11), orientin (compound 13), vitexin (compound 26), and naringin (compound 28). The remaining 24 compounds were tentatively identified (Level 2) through high-resolution tandem MS spectral matching against the mzCloud database (matching score >80), supported by their consistency with previously reported constituents of the component herbs.

The identified constituents included flavonoids, triterpenoids, and phenolic glycosides. Notable compounds included oleanolic acid (compound 4) and miquelianin (compound 7). These findings characterized the chemical composition of BJSE and identified candidate constituents for subsequent network pharmacology and molecular docking analyses.

### Identification of potential molecular targets associated with sperm motility

A total of 207 genes associated with spermatogenesis and sperm motility were retrieved from the GeneCards database. The compound–target interaction analysis identified 14 hub nodes potentially associated with the reproductive effects of BJSE (Figures 2A and B).

A PPI network comprising 14 nodes and 112 edges was constructed using the STRING database (Figure 2C). Network analysis highlighted interactions involving SRC, ESR1, ESR2, and AR (Figure 2D). The network topology results are summarized in Figure 2E and Table 2.

Hub gene analysis using the maximal clique centrality algorithm identified AR, ESR1, prostaglandin-endoperoxide synthase 2 (PTGS2), SRC, and tumor necrosis factor (TNF) among the principal candidate targets (Figure 2F).

Functional module enrichment indicated associations with steroid receptor coactivator activity and nuclear estrogen receptor activity. The response to steroid hormones was identified as a prominent enriched biological process (Figure 2G). These findings suggested that hormone-associated signaling networks were represented among the predicted molecular targets of BJSE.

### Functional enrichment analysis of candidate targets

GO enrichment analysis identified biological processes associated with the regulation of transcription by RNA polymerase II, estrogen receptor signaling, nuclear receptor-mediated steroid hormone signaling, and regulation of DNA biosynthesis (Figures 2H–J).

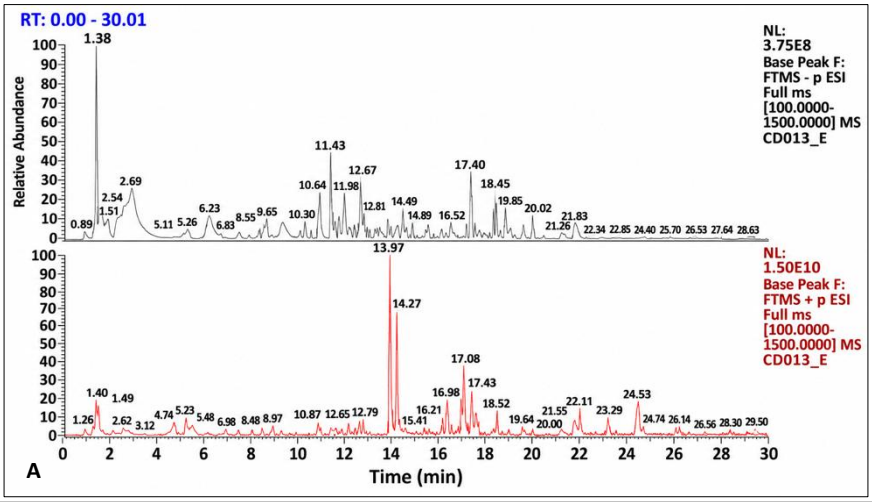
Enriched cellular components included protein-containing complexes, cytoplasm, intracellular membrane-bounded organelles, and caveolae. The principal enriched molecular functions included enzyme binding, transcription coactivator binding, identical protein binding, nuclear estrogen receptor activity, and heme binding. Enrichment significance was assessed after Benjamini–Hochberg false discovery rate correction.

KEGG pathway enrichment analysis identified several pathways associated with the candidate targets, including prolactin signaling, human cytomegalovirus infection, estrogen signaling, Rap1 signaling, and advanced

glycation end product–receptor for advanced glycation end product signaling (Figure 2K).

The 20 leading enriched pathways included hormone-related pathways, such as estrogen signaling, prolactin signaling, gonadotropin-releasing hormone secretion, and ovarian steroidogenesis; disease-associated pathways, including herpes simplex virus 1 infection, Yersinia infection, human cytomegalovirus infection, and type 2 diabetes mellitus; and signaling-related pathways, including Rap1, TNF, relaxin, and mitogen-activated protein kinase signaling (Figure 2L).

These enrichment results indicated that the predicted targets of BJSE were associated with multiple hormone-regulatory and intracellular signaling pathways. However, pathway enrichment alone did not establish functional activation or inhibition of these pathways following BJSE administration.




**Identification of chemical constituents from BJSE by UPLC-quadrupole-orbitrap MS**

| No. | tR(min) | Adducts | MS1 (m/z) | MS2 (m/z) | Error (ppm) | Molecular formula | Identity |
|---|---|---|---|---|---|---|---|
| 1 | 10.191 | [M-H]-1 | 525.16138 | 479.21, 357.12, 283.08, 195.07, 121.03 | -13.82 | $C_{29}H_{28}O_{11}$ | albiflorin |
| 2 | 14.608 | [M+H]+1 | 447.09122 | 217.06, 253.05, 235.05, 123.01, 103.05 | 15.80 | $C_{22}H_{18}O_{11}$ | Baicalin * |
| 3 | 14.569 | [M-H]-1 | 585.1958 | 261.11, 267.09, 249.05, 197.08, 105.03 | 12.46 | $C_{28}H_{34}O_{13}$ | {(3R,5R,6S,8S)-3-[(6-O-Benzoyl-β-D-glucopyranosyl)oxy]-6-hydroxy-8-methyl-9,10-dioxasteracyclo[4.3.1.$0^{2,5}$.$0^{3,8}$]dec-2-yl} methyl benzoate |
| 4 | 22.084 | [M+H]-1 | 453.35294 | 416.01, 227.20, 121.03, 112.98 | -16.02 | $C_{26}H_{28}O_{7}$ | Oleanolic acid * |
| 5 | 13.964 | [M+H]-1 | 463.05606 | 343.08, 287.05, 238.05, 213.05, 153.02 | 14.65 | $C_{23}H_{38}O_{12}$ | (2S,3S,4S,5R,6S)-6-[(5,7-dihydroxy-2-(4-hydroxyphenyl)-4-oxo-4H-chromene-3-yl)oxy}-3,4,5-trihydroxyoxane-2-carboxylic acid |
| 6 | 10.885 | [M+H]-1 | 479.15381 | 325.09, 307.08, 245.08, 230.07, 163.04 | 15.23 | $C_{23}H_{30}O_{11}$ | [(2R,3S,4S,5R,6R)-6-[2-(3,4-dihydroxyphenyl)ethoxy]-3,4,5-trihydroxyoxane-2-yl]methyl (2E)-3-(3,4-dihydroxyphenyl)prop-2-enoate * |
| 7 | 13.322 | [M-H]-1 | 477.06713 | 301.04, 273.04, 245.05, 179.90, 151.00 | -14.98 | $C_{20}H_{18}O_{13}$ | Miguelianin * |
| 8 | 13.244 | [M+H]+1 | 579.16998 | 433.11, 326.97, 271.06, 153.02, 119.05 | 12.57 | $C_{27}H_{30}O_{14}$ | 5-hydroxy-3-(4-hydroxyphenyl)-7-[(((2S,3R,4S,5S,6R)-3,4,5-trihydroxy-6-[{(2R,3R,4R,5R,6S)-3,4,5-trihydroxy-6-methyl)oxan-2-yl)oxy]methyl]oxan-2-yl)oxy}-4H-chromen-4-one |
| 9 | 15.426 | [M+H]+1 | 661.16707 | 255.08, 270.05, 242.06, 186.02, 168.01 | 15.34 | $C_{32}H_{30}O_{17}$ | (2S,3S,4S,5R,6S)-3,4,5-trihydroxy-6-[(5-hydroxy-3-methoxy-4-oxo-2-phenyl-4H-chromen-7-yl)oxy]ox ane-2-carboxylic acid |
| 10 | 16.773 | [M+H]-1 | 435.1283 | 273.08, 171.03, 153.02, 147.04, 119.05 | 16.77 | $C_{23}H_{22}O_{9}$ | Prunin |
| 11 | 21.074 | [M+H]-1 | 471.34668 | 317.21, 271.20, 235.17, 189.16, 149.10 | 15.41 | $C_{26}H_{40}O_{7}$ | 18-β-Glycyrrhetinic acid |
| 12 | 11.761 | [M+H]-1 | 449.10706 | 431.10, 329.07, 299.05, 271.06, 137.02 | 15.67 | $C_{22}H_{26}O_{11}$ | Ononin * |
| 13 | 10.886 | [M+H]-1 | 625.21118 | 471.15, 263.09, 243.07, 163.04, 135.01 | 11.65 | $C_{28}H_{36}O_{15}$ | 2-(3,4-Dihydroxyphenyl)ethyl 3-O-(6-deoxy-β-L-mannopyranosyl)-6-O-[(2E)-3-(3,4-dihydroxyphenyl)-2-propenoyl]-β-D-glucopyranoside |
| 14 | 11.938 | [M+H]-1 | 449.10693 | 413.09, 353.06, 329.07, 299.05, 165.02 | 15.91 | $C_{22}H_{26}O_{11}$ | (1S)-1,5-Anhydro-1-[2-(3,4-dihydroxyphenyl)-5,7-dihydroxy-4-oxo-4H-chromen-6-yl]-D-galactitol |
| 15 | 12.63 | [M+H]-1 | 433.11185 | 397.09, 337.07, 313.07, 283.06, 165.02 | 16.48 | $C_{22}H_{22}O_{10}$ | 1,5-Anhydro-1-[5,7-dihydroxy-2-(4-hydroxyphenyl)-4-oxo-4H-chromen-6-yl]besitol |
| 16 | 11.48 | [M+H]-1 | 611.19586 | 369.10, 345.10, 303.09, 177.05, 153.02 | 11.91 | $C_{32}H_{36}O_{13}$ | Hesperidin * |
| 17 | 12.193 | [M+H]-1 | 549.15942 | 495.13, 411.11, 355.09, 309.08, 279.07 | 12.81 | $C_{28}H_{34}O_{13}$ | 5,7-dihydroxy-2-phenyl-6-[3,4,5-trihydroxy-6-(hydroxymethyl)oxan-2-yl]-8-(3,4,5-trihydroxyoxan-2-yl)-4H-chromen-4-one |
| 18 | 13.687 | [M+H]-1 | 449.10763 | 329.07, 287.05, 213.05, 153.02, 121.03 | 15.69 | $C_{23}H_{28}O_{9}$ | Trifolin * |
| 19 | 11.988 | [M+H]-1 | 623.19713 | 461.17, 315.11, 161.02, 133.03, 113.02 | -11.63 | $C_{28}H_{36}O_{15}$ | 2-(3,4-Dihydroxyphenyl)ethyl 3-O-(6-deoxy-β-L-mannopyranosyl)-6-O-[(2E)-3-(3,4-dihydroxyphenyl)-2-propenoyl]-β-D-glucopyranoside |
| 20 | 15.445 | [M+H]-1 | 477.10196 | 301.07, 286.05, 241.05, 202.01, 184.09 | 14.58 | $C_{22}H_{22}O_{12}$ | 6-O-Methylssiicetularin * |
| 21 | 26.018 | [M+H]-1 | 447.34625 | 271.06, 219.17, 201.16, 167.03, 119.02 | 16.18 | $C_{23}H_{40}O_{8}$ | Dioctyl phthalate |
| 22 | 12.563 | [M-H]-1 | 433.11398 | 313.07, 271.06, 177.02, 151.00, 119.05 | -16.47 | $C_{23}H_{24}O_{9}$ | 7-Hydroxy-2-(4-hydroxyphenyl)-1-oxo-3,4-dihydro-2H-chromeno-5-yl β-D-glucopyranoside * |
| 23 | 13.586 | [M+H]+1 | 463.12308 | 301.07, 286.05, 238.05, 169.01, 153.02 | 15.75 | $C_{22}H_{24}O_{11}$ | 5-hydroxy-2-(4-hydroxyphenyl)-6-methoxy-7-[(1(2S,3R,4S,5S,6R)-3,4,5-trihydroxy-6-(hydroxymethyl)oxan-2-yl)oxy]-4H-chromen-4-one |
| 24 | 12.681 | [M-H]-1 | 623.19751 | 461.17, 297.10, 161.02, 133.03, 113.02 | -11.63 | $C_{28}H_{36}O_{15}$ | 2-(3,4-Dihydroxyphenyl)ethyl 3-O-(6-deoxy-β-L-mannopyranosyl)-6-O-[(2E)-3-(3,4-dihydroxyphenyl)-2-propenoyl]-β-D-glucopyranoside |
| 25 | 11.743 | [M+H]-1 | 545.15405 | 409.10, 379.09, 325.07, 299.06, 121.03 | 12.89 | $C_{26}H_{34}O_{13}$ | Cerythroside |
| 26 | 12.203 | [M+H]-1 | 433.11191 | 397.09, 313.07, 297.08, 283.06, 255.05 | 16.85 | $C_{21}H_{22}O_{10}$ | Vitexin |
| 27 | 10.179 | [M+H]+1 | 481.16995 | 315.12, 197.09, 151.08, 133.06, 105.03 | 15.12 | $C_{23}H_{28}O_{11}$ | [(3R,5R,6S,8S)-3-(β-D-Glucopyranosyloxy)-6-hydroxy-8-methyl-9,10-dioxatetracyclo[4.3.1.$0^{2,5}$.$0^{3,8}$]dec-2-yl]methyl benzoate |
| 28 | 12.44 | [M+H]-1 | 581.18524 | 273.08, 195.03, 153.02, 147.04, 85.03 | 11.86 | $C_{27}H_{30}O_{14}$ | Naringin * |
| 29 | 13.426 | [M+H]+1 | 433.11261 | 397.09, 313.07, 271.06, 187.04, 153.02 | 16.85 | $C_{22}H_{20}O_{10}$ | Apigetrin |

**Note:** * identified by authentic reference, others identified through database.

B

**Figure 1:** Chemical characterization of BAJISAN extract using ultra-high-performance liquid chromatography coupled with quadrupole-Orbitrap MS. (A) Base peak chromatograms acquired in positive-ion mode (upper panel) and negative-ion mode (lower panel). (B) Chemical constituents identified in the extract, including compounds confirmed using authentic reference standards and those tentatively identified through spectral database matching. BJSE = BAJISAN extract; UPLC = Ultra-high-performance liquid chromatography; MS = Mass spectrometry. Asterisks identify compounds confirmed using authentic reference standards (Level 1); the remaining compounds were tentatively identified (Level 2).

**Table 2:** Top 10 candidate molecular targets identified through protein–protein interaction network analysis, with corresponding network centrality parameters.

| Rank | Target | Betweenness centrality | Closeness centrality | Degree |
|---|---|---|---|---|
| 1 | TNF | 0.28461538 | 0.92857143 | 12 |
| 2 | ESR1 | 0.05705128 | 0.86666667 | 11 |
| 2 | AR | 0.05705128 | 0.86666667 | 11 |
| 4 | SRC | 0.03247863 | 0.81250000 | 10 |
| 5 | PTGS2 | 0.01196581 | 0.72222222 | 8 |
| 5 | FGF2 | 0.05277778 | 0.72222222 | 8 |
| 5 | PIK3CA | 0.02542735 | 0.68421052 | 8 |
| 8 | ESR2 | 0.00534188 | 0.68421053 | 7 |
| 9 | CYP19A1 | 0.00534188 | 0.68421053 | 7 |
| 10 | TERT | 0.00320513 | 0.64999999 | 6 |

AR = Androgen receptor; CYP19A1 = Cytochrome P450 family 19 subfamily A member 1; ESR1 = Estrogen receptor 1; ESR2 = Estrogen receptor 2; FGF2 = Fibroblast growth factor 2; PIK3CA = Phosphatidylinositol-4,5-bisphosphate 3-kinase catalytic subunit alpha; PTGS2 = Prostaglandin-endoperoxide synthase 2; SRC = SRC proto-oncogene, non-receptor tyrosine kinase; TERT = Telomerase reverse transcriptase; TNF = Tumor necrosis factor. Betweenness centrality represents the extent to which a node lies on shortest paths between other nodes; closeness centrality reflects the inverse average shortest-path distance to other nodes; degree indicates the number of direct network connections.

## Molecular docking analysis

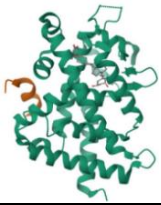
Five candidate constituents of BJSE—baicalin, hesperidin, oleanolic acid, orientin, and vitexin—were selected for molecular docking against AR, AURKA, ESR1, nuclear receptor subfamily 3 group C member 1 (NR3C1), and SRC (Table 3).

According to the reported docking interpretation criteria, predicted binding energies below −4.25 kcal/mol were considered indicative of potential ligand–target interactions, values below −5.0 kcal/mol indicated favorable predicted binding, and values below −7.0 kcal/mol indicated stronger predicted binding affinity [52].

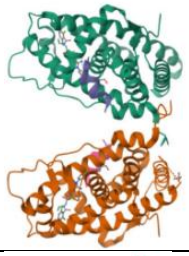
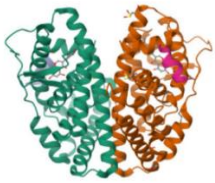
Several ligand–target combinations yielded docking energies below −7.0 kcal/mol. The reported interactions included baicalin–AR (−10.00 kcal/mol), baicalin–NR3C1 (−10.40 kcal/mol), hesperidin–AR (−8.80 kcal/mol), hesperidin–ESR1 (−8.80 kcal/mol), hesperidin–NR3C1 (−11.20 kcal/mol), oleanolic acid–AURKA (−9.08 kcal/mol), orientin–AR (−10.87 kcal/mol), orientin–SRC (−9.88 kcal/mol), and vitexin–NR3C1 (−7.53 kcal/mol) (Figures 2M–Q).

These docking results suggested favorable predicted interactions between selected BJSE constituents and reproductive signaling-associated proteins. However, the predicted binding energies did not independently confirm biochemical binding or functional modulation of the corresponding targets.

**Table 3:** Predicted molecular docking affinities of selected BAJISAN extract constituents with candidate target proteins.

| No. | Protein | PDB ID | Structure | Docking compound | Affinity (kcal/mol) |
|---|---|---|---|---|---|
| 1 | AR | 5XPN |  | baicalin<br>hesperidin<br>oleanolic acid<br>orientin<br>vitexin | –10<br>–8.8<br>–7.87<br>–10.87<br>–6.94 |
| 2 | AURKA | 5DPV |  | baicalin<br>hesperidin<br>oleanolic acid<br>orientin<br>vitexin | –9.7<br>–8.6<br>–9.08<br>–7.05<br>–6.77 |
| 3 | ESR1 | 4XI3 |  | baicalin<br>hesperidin<br>oleanolic acid<br>orientin<br>vitexin | –7.8<br>–8.8<br>–7.96<br>–7.26<br>–6.48 |

doi: 10.14202/vetworld.2026.5011-5034

| No. | Protein | PDB ID | Structure | Docking compound | Affinity (kcal/mol) |
|---|---|---|---|---|---|
| 4 | NR3C1 | 3E7C |  | baicalin<br>hesperidin<br>oleanolic acid<br>orientin<br>vitexin | –10.4<br>–11.2<br>–8.67<br>–8.98<br>–7.53 |
| 5 | NR3C1 | 4NH5 |  | baicalin<br>hesperidin<br>oleanolic acid<br>orientin<br>vitexin | –7.4<br>–6.2<br>–6.67<br>–6.98<br>–7.53 |
| 6 | SRC | 5JMM |  | baicalin<br>hesperidin<br>oleanolic acid<br>orientin<br>vitexin | –8.1<br>–7.2<br>–8.73<br>–9.88<br>–7.46 |

Values represent predicted docking binding energies (kcal/mol); more negative values indicate more favorable predicted binding under the applied docking model. AR = Androgen receptor; AURKA = Aurora kinase A; ESR1 = Estrogen receptor 1; NR3C1 = Nuclear receptor subfamily 3 group C member 1; SRC = SRC proto-oncogene, non-receptor tyrosine kinase; PDB = Protein Data Bank. The two NR3C1 entries correspond to different protein structures.

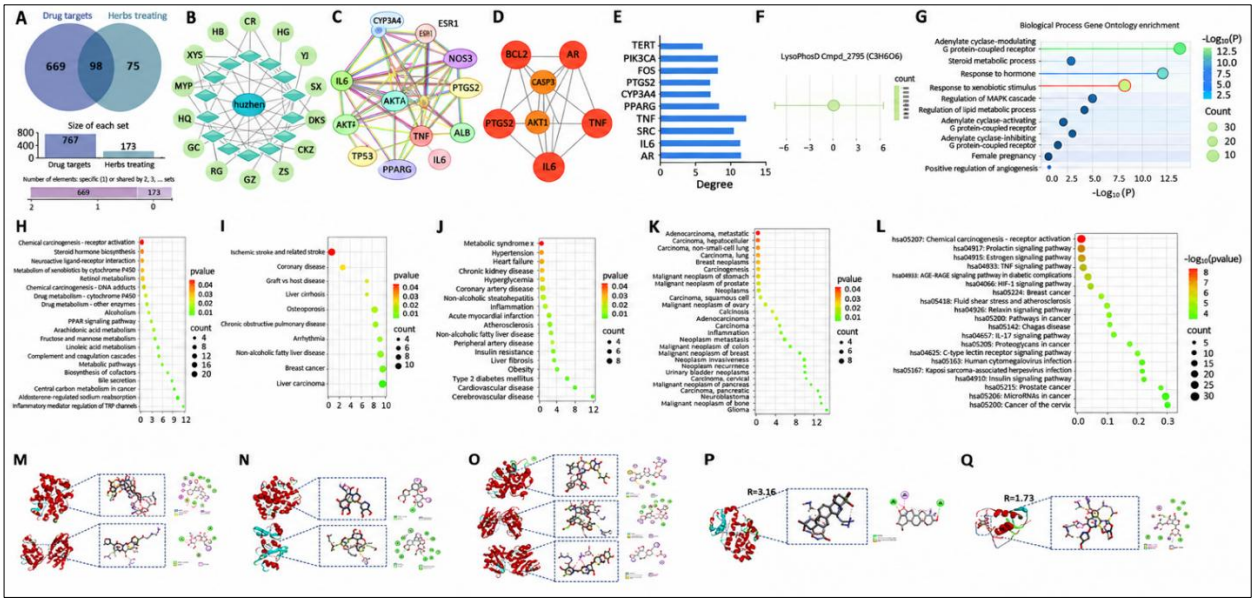



**Figure 2:** Network pharmacology, functional enrichment, and molecular docking analyses of candidate targets associated with the effects of BAJISAN extract on sperm motility. (A) Venn diagram of targets identified in at least two sperm motility-related searches. (B) Network of BJSE-associated candidate targets related to sperm motility. (C) Protein–protein interaction network of overlapping targets. (D) Eight hub genes identified through network analysis. (E) Degree-based ranking of the 10 leading overlapping targets. (F) Local network cluster identified using STRING. (G) GO biological process enrichment of the selected network targets. (H–J) GO enrichment results for biological processes, cellular components, and molecular functions, respectively. (K) Kyoto Encyclopedia of Genes and Genomes pathway enrichment analysis of overlapping targets. (L) Twenty leading enriched pathways. (M) Predicted docking interactions of baicalin with AR (−10.00 kcal/mol) and NR3C1 (−10.40 kcal/mol). (N) Orientin with AR (−10.87 kcal/mol) and SRC (−9.88 kcal/mol). (O) Hesperidin with AR (−8.80 kcal/mol), ESR1 (−8.80 kcal/mol), and NR3C1 (−11.20 kcal/mol). (P) Oleanolic acid with AURKA (−9.08 kcal/mol). (Q) Vitexin with NR3C1 (−7.53 kcal/mol). BJSE = BAJISAN extract; AR = Androgen receptor; AURKA = Aurora kinase A; ESR1 = Estrogen receptor 1; NR3C1 = Nuclear receptor subfamily 3 group C member 1; SRC = SRC proto-oncogene, non-receptor tyrosine kinase; PPI = Protein–protein interaction; GO = Gene Ontology; BP = Biological process; CC = Cellular component; MF = Molecular function; KEGG = Kyoto Encyclopedia of Genes and Genomes; STRING = Search Tool for the Retrieval of Interacting Genes/Proteins. Docking affinities are expressed in kcal/mol and represent computational predictions rather than experimentally confirmed binding.

### Effects of BJSE on sperm quality and motility

BJSE administration was associated with significant improvements in sperm quality parameters across the experimental period (Table 4). The high-dose group generally demonstrated the greatest improvements in sperm survival, acrosome integrity, and sperm morphology compared with the control group ($p < 0.05$).

At week 16, sperm survival increased from 72.81% ± 1.16% in the control group to 88.32% ± 1.73% in the BJSE-H group. Similarly, acrosome integrity increased from 53.21% ± 1.22% to 62.73% ± 0.45%, whereas the sperm deformity rate decreased from 8.55% ± 0.16% to 6.79% ± 0.35%.

Sperm motility classification also differed among treatment groups. At week 16, Grade A sperm accounted for 43.80% ± 0.85% in the BJSE-H group compared with 23.28% ± 1.26% in the control group. Grade D sperm decreased from 24.08% ± 1.42% in the control group to 8.55% ± 0.20% and 13.52% ± 0.21% in the BJSE-M and BJSE-H groups, respectively.

The study reported significant linear dose-response trends for the principal sperm quality parameters ($p < 0.05$). At week 16, comparisons between the BJSE-H and control groups yielded large standardized effect sizes for sperm survival (Cohen's d = 4.30), acrosome integrity (d = 4.23), deformity rate (d = −2.64), and Grade A sperm proportion (d = 7.80).

At week 16, Cohen's d values (95% confidence intervals) for BJSE-H versus control were: survival rate, 4.30 (2.12–6.41); intact acrosome rate, 4.23 (2.04–6.34); deformity rate, −2.64 (−4.81 to −0.51); Grade A, 7.80 (4.03–11.57); Grade B, −1.76 (−3.28 to −0.25); Grade C, −2.37 (−4.05 to −0.69); and Grade D, −4.25 (−6.57 to −1.93).

**Table 4:** Effects of BAJISAN extract administration on sperm survival, acrosome integrity, morphological abnormalities, and motility grades in rabbits.

| Week | Group | Survival (%) | Intact acrosome (%) | Deformity (%) | Grade A (%) | Grade B (%) | Grade C (%) | Grade D (%) |
|---|---|---|---|---|---|---|---|---|
| 10 | Control | 75.88 ± 1.25$^{d}$ | 53.16 ± 1.64$^{c}$ | 8.84 ± 0.35$^{a}$ | 22.08 ± 0.48$^{d}$ | 26.29 ± 1.72$^{b}$ | 26.13 ± 1.34$^{b}$ | 25.48 ± 1.44$^{a}$ |
| 10 | BJSE-L | 81.43 ± 0.70$^{c}$ | 54.42 ± 2.02$^{bc}$ | 8.45 ± 0.19$^{ab}$ | 31.12 ± 1.07$^{c}$ | 26.05 ± 2.49$^{b}$ | 28.17 ± 1.48$^{a}$ | 14.67 ± 2.20$^{b}$ |
| 10 | BJSE-M | 84.20 ± 2.13$^{b}$ | 57.42 ± 1.73$^{ab}$ | 8.29 ± 0.40$^{b}$ | 35.80 ± 0.87$^{b}$ | 31.08 ± 1.05$^{a}$ | 22.53 ± 0.93$^{c}$ | 10.57 ± 1.46$^{c}$ |
| 10 | BJSE-H | 89.64 ± 1.75$^{a}$ | 58.61 ± 1.31$^{a}$ | 8.01 ± 0.24$^{b}$ | 43.21 ± 0.93$^{a}$ | 21.32 ± 0.88$^{c}$ | 19.56 ± 0.94$^{d}$ | 15.90 ± 2.10$^{b}$ |
| 12 | Control | 72.70 ± 1.76$^{c}$ | 53.64 ± 1.36$^{c}$ | 8.27 ± 0.22$^{a}$ | 24.17 ± 1.89$^{d}$ | 26.48 ± 0.61$^{a}$ | 25.19 ± 1.48$^{ab}$ | 24.15 ± 3.71$^{a}$ |
| 12 | BJSE-L | 83.30 ± 0.91$^{b}$ | 54.62 ± 0.90$^{bc}$ | 8.03 ± 0.34$^{ab}$ | 34.39 ± 0.64$^{c}$ | 23.41 ± 1.66$^{b}$ | 27.17 ± 0.91$^{a}$ | 14.91 ± 1.91$^{b}$ |
| 12 | BJSE-M | 83.73 ± 1.31$^{b}$ | 56.05 ± 2.21$^{b}$ | 8.02 ± 0.14$^{ab}$ | 36.33 ± 0.98$^{b}$ | 28.03 ± 0.97$^{a}$ | 24.39 ± 0.86$^{b}$ | 11.24 ± 1.92$^{b}$ |
| 12 | BJSE-H | 88.99 ± 1.38$^{a}$ | 60.61 ± 0.69$^{a}$ | 7.82 ± 0.16$^{b}$ | 43.97 ± 1.18$^{a}$ | 22.89 ± 1.01$^{b}$ | 21.46 ± 1.84$^{c}$ | 11.69 ± 2.81$^{b}$ |
| 14 | Control | 75.42 ± 1.72$^{c}$ | 52.68 ± 1.71$^{d}$ | 8.73 ± 0.33$^{a}$ | 22.62 ± 1.84$^{c}$ | 25.25 ± 1.09$^{d}$ | 25.25 ± 1.29$^{b}$ | 26.98 ± 2.68$^{a}$ |
| 14 | BJSE-L | 85.53 ± 1.79$^{b}$ | 56.30 ± 1.42$^{c}$ | 7.55 ± 0.54$^{b}$ | 36.14 ± 1.57$^{b}$ | 25.27 ± 0.70$^{b}$ | 27.44 ± 0.66$^{a}$ | 11.16 ± 0.79$^{c}$ |
| 14 | BJSE-M | 85.28 ± 2.20$^{b}$ | 58.31 ± 0.36$^{b}$ | 7.38 ± 0.39$^{b}$ | 37.47 ± 1.59$^{b}$ | 28.76 ± 1.03$^{a}$ | 23.83 ± 0.70$^{c}$ | 9.95 ± 0.19$^{c}$ |
| 14 | BJSE-H | 89.55 ± 1.75$^{a}$ | 62.42 ± 0.70$^{a}$ | 7.38 ± 0.29$^{b}$ | 44.53 ± 0.38$^{a}$ | 21.29 ± 1.22$^{c}$ | 19.72 ± 0.43$^{d}$ | 14.47 ± 0.55$^{b}$ |
| 16 | Control | 72.81 ± 1.16$^{c}$ | 53.21 ± 1.22$^{d}$ | 8.55 ± 0.16$^{a}$ | 23.28 ± 1.26$^{d}$ | 26.18 ± 0.88$^{b}$ | 26.47 ± 1.20$^{a}$ | 24.08 ± 1.42$^{a}$ |
| 16 | BJSE-L | 86.30 ± 2.21$^{ab}$ | 56.08 ± 0.46$^{c}$ | 7.28 ± 0.17$^{b}$ | 36.15 ± 0.44$^{c}$ | 27.34 ± 1.32$^{b}$ | 26.30 ± 1.06$^{a}$ | 10.08 ± 0.95$^{c}$ |
| 16 | BJSE-M | 85.58 ± 2.03$^{b}$ | 59.99 ± 1.03$^{b}$ | 7.02 ± 0.22$^{bc}$ | 38.81 ± 0.91$^{b}$ | 29.21 ± 1.68$^{a}$ | 23.44 ± 1.07$^{b}$ | 8.55 ± 0.20$^{d}$ |
| 16 | BJSE-H | 88.32 ± 1.73$^{a}$ | 62.73 ± 0.45$^{a}$ | 6.79 ± 0.35$^{c}$ | 43.80 ± 0.85$^{a}$ | 22.73 ± 0.71$^{c}$ | 19.95 ± 1.04$^{c}$ | 13.52 ± 0.21$^{b}$ |

Values are presented as mean ± standard error of the mean (n = 6 rabbits/group). Different superscript letters within the same week and outcome column indicate statistically significant differences ($p < 0.05$), as reported by the authors. BJSE = BAJISAN extract; BJSE-L = Low-dose BJSE (150 mg/kg body weight); BJSE-M = Medium-dose BJSE (300 mg/kg); BJSE-H = High-dose BJSE (600 mg/kg). Grades A–D represent rapid progressive, slow progressive, nonprogressive, and immotile spermatozoa, respectively.

### Effects on sperm kinematic parameters

BJSE administration improved several sperm kinematic parameters throughout the experimental period (Table 5). Compared with the control group, medium- and high-dose treatments generally increased VAP, VCL, VSL, and BCF ($p < 0.05$).

At week 16, VAP increased from 10.15 ± 0.29 in the control group to 17.07 ± 0.68 in the BJSE-H group. Corresponding increases were observed in VCL (16.73 ± 0.34 to 27.21 ± 1.44), VSL (6.26 ± 0.48 to 12.30 ± 0.41), and BCF (9.30 ± 0.11 to 11.12 ± 0.17).

The MAD exhibited a different response pattern. At week 16, MAD was lower in the BJSE-M and BJSE-H groups than in the control group ($p < 0.05$). Amplitude of lateral head displacement (ALH) was highest in the BJSE-M group at the final assessment.

The week 16 effect sizes for VAP, VCL, VSL, and BCF were large, whereas the confidence intervals for MAD and ALH included zero. Overall, the findings indicated that BJSE administration was associated with improvements in several, but not all, sperm kinematic measurements.

At week 16, Cohen's d values (95% confidence intervals) for BJSE-H versus control were: VAP, 5.41 (3.01–7.90); VCL, 4.09 (1.86–6.26); VSL, 5.53 (3.66–9.41); MAD, −1.23 (−2.71 to 0.17); ALH, 0.86 (−0.48 to 2.20); and BCF, 5.20 (2.51–7.89).

**Table 5:** Effects of BAJISAN extract administration on sperm kinematic parameters in rabbits.

| Week | Group | VAP (μm/s) | VCL (μm/s) | VSL (μm/s) | MAD (°) | ALH (μm) | BCF (Hz) |
|---|---|---|---|---|---|---|---|
| 10 | Control | 10.41 ± 0.56$^{b}$ | 16.57 ± 0.37$^{d}$ | 6.14 ± 0.39$^{d}$ | 76.42 ± 2.19$^{c}$ | 1.97 ± 0.10$^{b}$ | 9.10 ± 0.26$^{c}$ |
| 10 | BJSE-L | 11.03 ± 0.46$^{b}$ | 19.32 ± 0.88$^{c}$ | 9.22 ± 0.40$^{c}$ | 81.62 ± 1.33$^{b}$ | 2.41 ± 0.15$^{a}$ | 10.10 ± 0.35$^{b}$ |
| 10 | BJSE-M | 16.85 ± 0.74$^{a}$ | 25.27 ± 1.14$^{b}$ | 11.67 ± 0.42$^{b}$ | 80.70 ± 1.03$^{b}$ | 2.59 ± 0.15$^{a}$ | 10.68 ± 0.27$^{a}$ |
| 10 | BJSE-H | 16.88 ± 1.36$^{a}$ | 27.03 ± 0.55$^{a}$ | 13.09 ± 0.36$^{a}$ | 86.27 ± 0.57$^{a}$ | 2.79 ± 0.17$^{a}$ | 10.65 ± 0.14$^{a}$ |
| 12 | Control | 10.78 ± 0.38$^{d}$ | 18.48 ± 0.48$^{c}$ | 6.68 ± 0.42$^{d}$ | 77.78 ± 3.28$^{ab}$ | 2.05 ± 0.06$^{c}$ | 9.27 ± 0.34$^{c}$ |
| 12 | BJSE-L | 13.24 ± 0.51$^{c}$ | 24.94 ± 0.64$^{b}$ | 9.58 ± 0.21$^{c}$ | 79.96 ± 1.13$^{a}$ | 2.45 ± 0.14$^{b}$ | 10.76 ± 0.31$^{b}$ |
| 12 | BJSE-M | 15.74 ± 0.64$^{b}$ | 27.65 ± 1.73$^{a}$ | 11.44 ± 0.59$^{b}$ | 75.57 ± 1.83$^{b}$ | 2.53 ± 0.17$^{ab}$ | 11.26 ± 0.62$^{ab}$ |
| 12 | BJSE-H | 17.48 ± 0.55$^{a}$ | 28.09 ± 0.88$^{a}$ | 12.60 ± 0.54$^{a}$ | 74.62 ± 2.07$^{b}$ | 2.70 ± 0.13$^{b}$ | 11.87 ± 0.69$^{a}$ |
| 14 | Control | 10.32 ± 0.39$^{c}$ | 17.16 ± 0.56$^{d}$ | 6.18 ± 0.41$^{d}$ | 77.69 ± 2.93$^{ab}$ | 2.04 ± 0.13$^{b}$ | 9.27 ± 0.21$^{b}$ |
| 14 | BJSE-L | 13.71 ± 0.89$^{b}$ | 21.12 ± 1.16$^{c}$ | 9.80 ± 0.77$^{c}$ | 79.34 ± 1.29$^{a}$ | 2.43 ± 0.05$^{a}$ | 10.76 ± 0.28$^{a}$ |
| 14 | BJSE-M | 16.97 ± 0.18$^{a}$ | 26.16 ± 1.20$^{b}$ | 11.45 ± 0.80$^{b}$ | 74.23 ± 3.08$^{bc}$ | 2.59 ± 0.14$^{a}$ | 11.06 ± 0.62$^{a}$ |
| 14 | BJSE-H | 17.19 ± 0.58$^{a}$ | 26.93 ± 0.94$^{a}$ | 12.44 ± 0.55$^{a}$ | 70.83 ± 1.90$^{c}$ | 2.56 ± 0.15$^{a}$ | 11.11 ± 0.48$^{a}$ |
| 16 | Control | 10.15 ± 0.29$^{c}$ | 16.73 ± 0.34$^{c}$ | 6.26 ± 0.48$^{d}$ | 77.80 ± 2.95$^{a}$ | 2.08 ± 0.14$^{c}$ | 9.30 ± 0.11$^{c}$ |
| 16 | BJSE-L | 14.05 ± 0.74$^{b}$ | 21.39 ± 1.51$^{b}$ | 10.05 ± 0.45$^{c}$ | 78.20 ± 1.28$^{a}$ | 2.39 ± 0.14$^{b}$ | 10.69 ± 0.29$^{b}$ |
| 16 | BJSE-M | 16.88 ± 0.45$^{a}$ | 25.96 ± 1.30$^{a}$ | 11.38 ± 0.42$^{b}$ | 74.28 ± 2.15$^{b}$ | 2.67 ± 0.19$^{a}$ | 11.27 ± 0.53$^{a}$ |
| 16 | BJSE-H | 17.07 ± 0.68$^{a}$ | 27.21 ± 1.44$^{a}$ | 12.30 ± 0.41$^{a}$ | 70.86 ± 1.38$^{c}$ | 2.42 ± 0.18$^{b}$ | 11.12 ± 0.17$^{ab}$ |

Values are presented as mean ± standard error of the mean (n = 6 rabbits/group); VAP/VCL/VSL in μm/s, MAD in degrees, ALH in μm, BCF in Hz. Different superscript letters within the same week and parameter column indicate significant differences ($p < 0.05$), as reported by the authors. BJSE = BAJISAN extract; BJSE-L = Low-dose BJSE (150 mg/kg); BJSE-M = Medium-dose BJSE (300 mg/kg); BJSE-H = High-dose BJSE (600 mg/kg); VAP = Average path velocity; VCL = Curvilinear velocity; VSL = Straight-line velocity; MAD = Mean angular displacement; ALH = Amplitude of lateral head displacement; BCF = Beat-cross frequency. Measurement units were not specified in the supplied table and require confirmation.

### Effects of BJSE on serum reproductive hormone concentrations

Serum FSH, LH, and testosterone concentrations were assessed to determine treatment-associated endocrine changes (Table 6).

**Table 6:** Effects of BAJISAN extract administration on serum reproductive hormone concentrations in rabbits.

| Week | Group | FSH (mIU/mL) | LH (mIU/mL) | Testosterone (ng/mL) |
|---|---|---|---|---|
| 8 | Control | 0.33 ± 0.03$^{b}$ | 3.64 ± 0.31$^{d}$ | 14.58 ± 1.38$^{d}$ |
| 8 | BJSE-L | 0.33 ± 0.03$^{b}$ | 4.52 ± 0.38$^{c}$ | 17.78 ± 0.90$^{c}$ |
| 8 | BJSE-M | 0.32 ± 0.02$^{b}$ | 5.05 ± 0.51$^{b}$ | 26.92 ± 0.93$^{b}$ |
| 8 | BJSE-H | 0.49 ± 0.03$^{a}$ | 5.72 ± 0.39$^{a}$ | 34.91 ± 0.66$^{a}$ |
| 16 | Control | 0.58 ± 0.06$^{a}$ | 3.85 ± 0.27$^{b}$ | 12.28 ± 0.80$^{b}$ |
| 16 | BJSE-L | 0.59 ± 0.03$^{a}$ | 4.39 ± 0.36$^{ab}$ | 13.20 ± 1.07$^{b}$ |
| 16 | BJSE-M | 0.38 ± 0.05$^{b}$ | 5.20 ± 0.61$^{a}$ | 13.57 ± 1.62$^{b}$ |
| 16 | BJSE-H | 0.42 ± 0.03$^{b}$ | 5.61 ± 1.08$^{a}$ | 18.05 ± 1.44$^{a}$ |

Values are presented as mean ± standard error of the mean (n = 6 rabbits/group). Different superscript letters within the same week and hormone column indicate significant differences ($p < 0.05$), as reported by the authors. BJSE = BAJISAN extract; BJSE-L = Low-dose BJSE (150 mg/kg); BJSE-M = Medium-dose BJSE (300 mg/kg); BJSE-H = High-dose BJSE (600 mg/kg); FSH = Follicle-stimulating hormone; LH = Luteinizing hormone; mIU/mL = Milli-international units per milliliter.

Two-way repeated-measures ANOVA identified significant treatment × time interactions for FSH ($F = 3.91$, $p = 0.002$), LH ($F = 4.82$, $p < 0.001$), and testosterone ($F = 5.34$, $p < 0.001$), indicating that differences among treatment groups varied with sampling time.

At week 8, the BJSE-H group exhibited significantly higher FSH (0.49 ± 0.03 mIU/mL), LH (5.72 ± 0.39 mIU/mL), and testosterone (34.91 ± 0.66 ng/mL) concentrations than the control group (0.33 ± 0.03 mIU/mL, 3.64 ± 0.31 mIU/mL, and 14.58 ± 1.38 ng/mL, respectively; $p < 0.05$). Significant positive linear dose-response trends were also reported for these hormones at week 8 ($p < 0.05$).

At week 16, significant between-group differences persisted for all three hormones, although the direction of the differences varied by analyte: FSH was lower in the BJSE-M and BJSE-H groups than in the control group, whereas LH and testosterone remained higher in the medium- and high-dose groups. Testosterone was significantly higher in the BJSE-H group (18.05 ± 1.44 ng/mL) than in the control group (12.28 ± 0.80 ng/mL).

These findings demonstrated time-dependent differences in reproductive hormone concentrations following BJSE administration. However, the hormonal measurements alone reflect treatment-associated changes in reproductive hormone concentrations rather than acceleration of sexual maturation, because the rabbits were already sexually mature at enrollment.

Treatment × time interactions were significant for FSH ($F = 3.91$, $p = 0.002$), LH ($F = 4.82$, $p < 0.001$), and testosterone ($F = 5.34$, $p < 0.001$).

**Testicular histology and expression of signaling-related genes and proteins**

Qualitative examination of hematoxylin- and eosin-stained testicular sections revealed spermatogenic cells at different developmental stages in all experimental groups, including spermatogonia, primary and secondary spermatocytes, spermatids, and mature spermatozoa (Figure 3A).

Spermatogonia were observed near the basement membrane of the seminiferous tubules, whereas more differentiated germ cells were located toward the tubular lumen. No marked abnormalities were described in the interstitial or connective tissues.

Compared with control sections, testicular sections from BJSE-treated rabbits appeared to have a more densely organized seminiferous epithelium and more tubules containing mature spermatozoa. These observations were qualitative, and no quantitative morphometric comparisons were performed.

qPCR analysis demonstrated significantly reduced *PTEN* expression and increased *mTOR*, *AKT1*, and *HSPA2* expression in testicular tissues from BJSE-treated rabbits ($p < 0.05$; Figure 3B).

Western blot analysis showed corresponding changes at the protein level, with significantly lower PTEN abundance and higher mTOR, Akt1, and HSPA2 abundance following BJSE treatment ($p < 0.05$; Figure 3C).

Significant linear dose-response trends were reported for these molecular measurements ($p < 0.05$). The coordinated transcript and protein expression changes were associated with the observed improvements in semen quality. However, these findings did not independently demonstrate activation of the signaling pathway or establish a causal relationship between the molecular changes and sperm function.

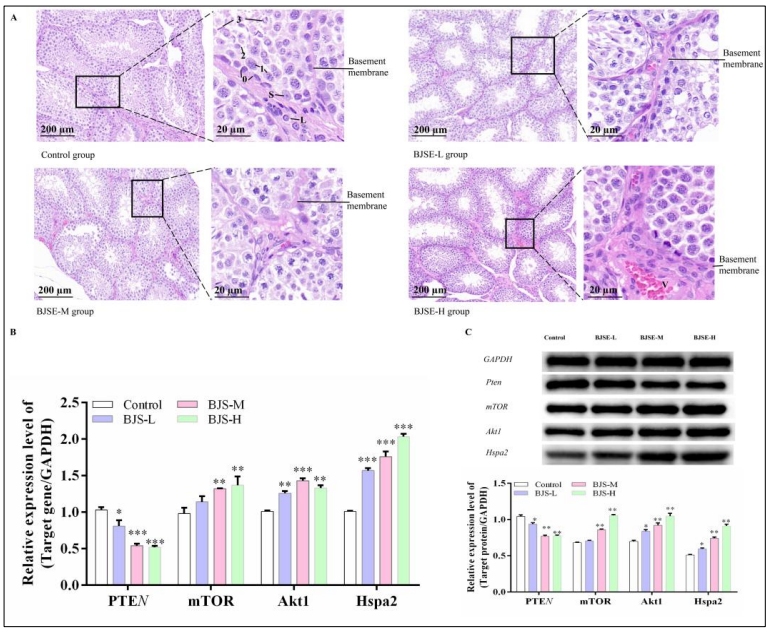



**Figure 3:** Testicular histological characteristics and expression of signaling-related genes and proteins in rabbits following BAJISAN extract administration. (A) Representative hematoxylin- and eosin-stained testicular sections showing seminiferous tubule architecture and spermatogenic cell populations (400× magnification; Scale bars = 200 μm). Labels indicate spermatogonia (0), primary spermatocytes (1), sperm cells (2), mature spermatozoa (3), supporting cells (S), interstitial cells (L), and blood vessels (V). (B) Relative messenger RNA expression of *PTEN*, *mTOR*, *AKT1*, and *HSPA2* determined by quantitative real-time polymerase chain reaction; relative expression was calculated using the 2^−ΔΔCt method with GAPDH as the reference gene. (C) Relative protein expression of PTEN, mTOR, Akt1, and HSPA2 determined by Western blot analysis; band intensities were normalized to β-actin. BJSE administration decreased PTEN expression and increased mTOR, Akt1, and HSPA2 expression compared with the control group. Data are presented as mean ± standard error of the mean (SEM) (n = 6 rabbits/group). BJSE = BAJISAN extract; PTEN = Phosphatase and tensin homolog; mTOR = Mechanistic target of rapamycin; AKT1 = AKT serine/threonine kinase 1; HSPA2 = Heat shock protein family A member 2. Gene symbols are italicized, whereas protein names are presented in roman type. Statistical significance: *$p < 0.05$, **$p < 0.01$, and ***$p < 0.001$.

## DISCUSSION

### Chemical composition and potential reproductive activities of BJSE

This study integrated chemical profiling, network pharmacology, molecular docking, and *in vivo* evaluation to investigate the effects of BJSE on semen quality and reproductive function in rabbits. BJSE administration was associated with improvements in sperm survival, motility, acrosome integrity, and morphology, accompanied by changes in reproductive hormone concentrations and testicular expression of signaling-related genes and proteins. These findings provide evidence of dose-associated reproductive effects and identify potential molecular mechanisms that warrant further investigation.

Ultra-high-performance liquid chromatography coupled with quadrupole-Orbitrap MS (UPLC-Q-Orbitrap MS) identified 29 major chemical constituents in BJSE, including flavonoids, triterpenoids, and phenolic glycosides. The identified compounds included baicalin, oleanolic acid, miquelianin, hesperidin, orientin, vitexin, and naringin. This chemical characterization provides a preliminary compositional profile that may support future investigations into formulation consistency and quality standardization.

Several identified constituents have previously been investigated for biological activities relevant to male reproductive function. Baicalin exhibits antioxidant and anti-inflammatory properties that may protect testicular germ cells against oxidative damage [53, 54]. Oleanolic acid has been associated with reduced germ cell DNA damage and apoptosis in experimental models of testicular dysfunction [55]. Hesperidin has been reported to improve sperm concentration and motility through antioxidant mechanisms and changes in reproductive hormone regulation [56, 57]. Vitexin and orientin have also demonstrated protective effects against testicular toxicity, potentially involving antioxidant and antiapoptotic activities [58]. However, the present study did not directly assess oxidative stress biomarkers, antioxidant enzyme activities, or apoptosis-related endpoints. Consequently, the relative contributions of these mechanisms remain uncertain.

These compounds suggest that multiple constituents may contribute to the reproductive effects associated with BJSE administration. Based on previous literature, antioxidant and antiapoptotic mechanisms have been proposed to operate independently of, or alongside, changes in phosphatase and tensin homolog (PTEN)/mTOR/AKT serine/threonine kinase 1 (Akt1) signaling. However, these mechanisms were not evaluated in the present study. Consequently, the relative contributions of these mechanisms remain uncertain.

Furthermore, because the complete herbal formulation was administered without comparison with individual compounds or defined combinations, the effects of specific constituents and potential synergistic interactions could not be established. These possibilities require direct experimental evaluation.

### Network pharmacology predictions and molecular docking findings

Network pharmacology and molecular docking provided a computational framework for identifying potential interactions between BJSE constituents and proteins involved in reproductive regulation. The analyses highlighted AR, ESR1, SRC proto-oncogene, non-receptor tyrosine kinase (SRC), and AURKA as candidate molecular targets. Functional enrichment further identified hormone-associated signaling pathways and other intracellular regulatory networks.

These findings are consistent with the multicomponent and multitarget characteristics frequently attributed to TCM formulations [27, 28]. Previous studies have investigated antioxidant and hormone-regulating effects of herbal preparations used for reproductive disorders [17, 19, 54]. This analysis extends this approach by identifying candidate proteins and predicted compound–target interactions for experimental investigation.

AR plays an essential role in male reproductive function through its involvement in Sertoli cell activity and spermatogenesis [36]. Molecular docking predicted favorable interactions between AR and several BJSE constituents, including baicalin, hesperidin, and orientin. These predictions, together with observed differences in serum testosterone concentrations, suggest that androgen-related signaling may be relevant to BJSE-associated reproductive responses. Nevertheless, we did not directly measure receptor binding or AR signaling activity.

SRC participates in intracellular signal transduction, cell adhesion, blood–testis barrier remodeling, and communication between Sertoli cells and developing germ cells [43, 44]. ESR1 contributes to fluid reabsorption, steroidogenic regulation, and spermatogenesis [38, 40]. Altered estrogen signaling has also been implicated in male reproductive dysfunction [39]. The predicted interaction between hesperidin and ESR1 therefore represents a potential mechanism for further investigation, rather than evidence that BJSE directly regulates estrogen receptor activity.

AURKA contributes to centrosome maturation and chromosome segregation during cell division, including

meiotic processes [37]. The predicted interaction between oleanolic acid and AURKA identifies another candidate target, although meiotic regulation and chromosome segregation were not evaluated experimentally.

The docking protocol yielded RMSD values below 2.0 Å for the re-docked native ligands, indicating that the docking procedure was technically reproducible under the selected conditions. However, favorable docking energies do not establish direct biochemical binding, target engagement, or functional effects *in vivo*.

Another methodological consideration is that we used human databases for target prediction, whereas the experimental investigation was conducted in rabbits. This approach was informed by the conservation of major reproductive signaling pathways among mammals. Nevertheless, formal ortholog mapping and sequence identity analyses were not performed, and species-specific differences in target regulation cannot be excluded.

Therefore, the computational findings should be interpreted as hypothesis-generating evidence that complements, but does not replace, experimental assessment of molecular mechanisms.

**Association between PTEN/mTOR/Akt1 expression and reproductive outcomes**

A key molecular finding was that BJSE administration was associated with reduced testicular PTEN expression and increased mTOR and Akt1 expression. These changes were observed at both messenger RNA and total protein levels and were accompanied by improvements in several semen quality parameters.

PTEN is an important negative regulator of PI3K/Akt signaling. This signaling network contributes to cellular survival, proliferation, metabolism, and spermatogenic regulation [32, 33, 59]. Previous experimental research has demonstrated the involvement of PI3K/Akt/mTOR signaling in reproductive tissue responses. For example, Long *et al.* [33] reported that retinoic acid was associated with restoration of spermatogenesis through modulation of this signaling pathway in a cryptorchid rat model.

The present findings are consistent with an association between BJSE administration and changes in expression of components of the PTEN/mTOR/Akt1 signaling network. However, reduced PTEN abundance and increased total Akt1 and mTOR abundance do not independently demonstrate increased pathway activity. Akt and mTOR activation is regulated by phosphorylation and other molecular processes not evaluated in this study.

Consequently, the observed expression changes do not definitively show that BJSE activated PI3K/Akt/mTOR signaling or that PTEN inhibition improved sperm quality. Confirmation would require measuring phosphorylated Akt and mTOR, assessing downstream signaling activity, and performing functional intervention experiments. These expression changes are therefore reported as molecular correlates of BJSE administration and should not be interpreted as evidence of pathway activation.

The histological observations provide additional context for the molecular findings. Testicular sections from BJSE-treated rabbits appeared to exhibit more densely organized seminiferous epithelium and more seminiferous tubules containing mature spermatozoa than control sections. These observations were consistent with improved semen quality.

Nevertheless, the histological evaluation was qualitative, and quantitative measurements of seminiferous tubule dimensions, epithelial thickness, or spermatogenic cell populations were not performed. Therefore, the apparent morphological differences provide descriptive support but cannot establish a quantitative increase in spermatogenic activity.

**Potential contribution of HSPA2 to sperm maturation and motility**

Heat shock protein family A member 2 (HSPA2) is a molecular chaperone involved in germ cell development, sperm maturation, capacitation, and sperm–oocyte interactions [45, 46]. In the present study, BJSE administration increased testicular HSPA2 messenger RNA and protein expression and improved sperm motility, acrosome integrity, and morphology.

Previous investigations have demonstrated the importance of HSPA2 in male reproductive function. Reduced HSPA2 abundance has been associated with impaired sperm maturation, diminished motility, and fertilization-related abnormalities [45]. Nixon *et al.* [46] demonstrated the involvement of HSPA2 in the organization of sperm surface proteins associated with sperm–zona pellucida interactions.

In addition, cellular stress responses may influence HSPA2 expression and sperm function. Oxidative stress has been associated with mitochondrial DNA damage and impaired sperm function [54, 60]. The presence of phytochemicals with previously reported antioxidant activities in BJSE raises the possibility that changes in cellular oxidative status may contribute to the observed HSPA2 response [61]. Nevertheless, the present study did not measure oxidative stress markers or directly assess HSPA2 function.

Sabeti *et al.* [53] reported lower HSPA2 abundance in spermatozoa from men with asthenozoospermia than

in those from normozoospermic controls, with a positive association between HSPA2 abundance and sperm motility. This finding provides additional biological context for the relationship between HSPA2 and sperm function.

Nevertheless, the present study did not measure oxidative stress markers or directly assess HSPA2 function. Furthermore, although HSPA2 and PTEN/mTOR/Akt1 expression changed in the same treatment groups, no direct published evidence currently establishes HSPA2 as a downstream effector of this signaling axis in rabbit testes, and a direct regulatory relationship between these proteins was not demonstrated in the present study. Available evidence from other species is limited to parallel expression changes rather than mechanistic upstream–downstream validation.

Thus, increased HSPA2 expression is a plausible molecular correlate of the observed improvements in sperm quality, not confirmation of a specific downstream mechanism.

**Effects of BJSE on reproductive hormone concentrations**

BJSE administration was associated with time-dependent changes in serum FSH, LH, and testosterone concentrations. Significant treatment × time interactions indicated that hormonal responses differed across the experimental period.

At week 8, the high-dose group exhibited significantly higher FSH, LH, and testosterone concentrations than the control group. These differences were accompanied by significant positive dose-response trends for the evaluated hormones. Testosterone is essential for spermatogenesis and Sertoli cell function, whereas FSH and LH contribute to the regulation of testicular development and reproductive endocrine activity [62].

These findings suggest that BJSE administration may influence reproductive hormone regulation. However, the hormonal response was not uniform across the study period.

At week 16, FSH concentrations were lower in the medium- and high-dose groups than in the control group, whereas LH concentrations remained higher in these groups. Testosterone also remained significantly higher in the high-dose group. Therefore, significant between-group differences persisted for all three hormones at week 16, although the direction of these differences varied by analyte.

Although the earlier hormonal differences could reflect treatment-associated changes in reproductive development, because the rabbits were already sexually mature at enrollment (7 months of age), the hormonal changes cannot be attributed to accelerated puberty; they are better interpreted as treatment-associated modulation of reproductive hormone concentrations. The study did not include independent assessments of pubertal progression or direct measurements of hypothalamic–pituitary–gonadal axis activity.

Accordingly, the endocrine findings should be interpreted as treatment- and time-associated changes in reproductive hormone concentrations rather than definitive evidence of accelerated puberty or sustained endocrine stimulation.

**Effects of BJSE on sperm motility and kinematic characteristics**

The improvements in semen quality were accompanied by changes in sperm kinematic parameters. BJSE administration generally increased VAP, VCL, VSL, and BCF, particularly in the medium- and high-dose groups.

These measurements reflect different aspects of sperm movement and provide information beyond conventional estimates of total motility. Increases in VAP and VSL indicate higher average path and straight-line displacement rates, whereas VCL reflects velocity along the sperm's actual trajectory.

The high-dose group exhibited consistently higher VSL than the control group across the evaluated time points. This finding is consistent with a higher proportion of spermatozoa exhibiting rapid progressive movement, as defined by the CASA velocity criteria.

However, MAD demonstrated a different pattern. At later sampling points, the medium- and high-dose groups generally exhibited lower MAD values than the control group. The amplitude of lateral head displacement (ALH) also varied among treatment groups and did not demonstrate a uniform dose-dependent increase.

Sperm movement patterns are influenced by multiple physiological processes. Hyperactivated motility, characterized by changes in flagellar movement and trajectory, contributes to fertilization-related functions but differs from progressive movement during sperm transport [18, 46, 63].

The combination of increased VSL and altered MAD observed in the present study reflects changes in sperm trajectory and velocity parameters; their functional significance remains to be determined. Nevertheless, reduced MAD alone cannot establish improved movement coordination, advanced sperm maturation, or enhanced fertilization competence.

Similarly, although increased HSPA2 expression was associated with improvements in semen quality, the study did not directly demonstrate that HSPA2 mediated the observed kinematic changes. Additional assessments of sperm hyperactivation, capacitation, fertilization capacity, and targeted molecular interventions would be necessary to clarify these relationships.

**Study strengths and limitations**

An important strength of this study was the integration of high-resolution chemical characterization, computational target prediction, molecular docking, and longitudinal *in vivo* assessment. This approach enabled the identification of candidate chemical constituents and molecular targets alongside experimentally measured reproductive outcomes.

Including three BJSE doses and repeated semen assessments at weeks 10, 12, 14, and 16 provided information on treatment-associated differences across doses and time points. Evaluating reproductive hormones, testicular histology, and gene and protein expression further supported a multidimensional assessment of reproductive function.

However, several limitations should be considered. First, the study included 24 rabbits, with six animals per group, and no formal *a priori* sample-size calculation was performed. This relatively small sample size may limit the precision and generalizability of the findings.

Second, the study used one batch of the complete BJSE formulation. The study did not investigate the effects of individual constituents, combinations of compounds, or potential synergistic interactions. Although the chemical constituents were characterized qualitatively, the study did not quantitatively standardize the principal compounds.

Third, network pharmacology predictions were based on human databases without formal human–rabbit ortholog mapping. Molecular docking was computational and did not establish direct target binding or functional modulation.

Fourth, molecular analyses measured messenger RNA and total protein abundance rather than phosphorylation status or pathway activity. Therefore, the study could not confirm activation of the PI3K/Akt/mTOR pathway or a causal relationship between molecular changes and reproductive improvements.

Fifth, testicular histology was evaluated qualitatively without quantitative morphometry. Oxidative stress, apoptosis, sperm capacitation, fertilization capacity, and reproductive success were not directly assessed.

Finally, several secondary outcomes were examined without a formal adjustment for multiple testing across all endpoints, increasing the possibility of chance findings. These limitations should be considered when interpreting the mechanistic and translational implications of the results.

**Future research directions**

Future studies should investigate BJSE effects in larger animal populations using prospectively calculated sample sizes and independently produced extract batches. Quantitative chemical profiling and identification of suitable marker compounds would support improved formulation standardization and reproducibility.

Further mechanistic investigations should assess phosphorylated Akt and mTOR, downstream signaling proteins, and functional pathway responses. Gene silencing, pharmacological inhibition, and rescue experiments could help determine whether changes in PTEN/mTOR/Akt1 signaling are necessary for the reproductive effects associated with BJSE.

The contribution of HSPA2 should also be evaluated through targeted functional experiments. In addition, antioxidant enzyme activity, oxidative stress biomarkers, apoptosis-related proteins, and mitochondrial function should be assessed to investigate alternative or complementary mechanisms.

Direct evaluation of selected phytochemicals and defined compound combinations would help distinguish the effects of individual constituents from those of the complete formulation. Experimental confirmation of predicted interactions involving AR, ESR1, SRC, and AURKA would also strengthen the interpretation of the network pharmacology findings.

Future reproductive investigations should incorporate quantitative testicular morphometry, sperm capacitation and fertilization assays, and breeding outcomes to establish whether improvements in semen parameters translate into enhanced reproductive performance.

**Overall interpretation**

The findings indicate that BJSE administration was associated with dose-dependent improvements in several

semen quality parameters, accompanied by changes in reproductive hormone concentrations and testicular expression of PTEN, mTOR, Akt1, and HSPA2. Chemical profiling and computational analyses identified candidate constituents and molecular targets that may contribute to these effects. The experimentally demonstrated contributions of this study are the dose-associated improvements in semen quality parameters and the changes in selected molecular markers (PTEN, mTOR, Akt1, and HSPA2 expression). The network pharmacology, molecular docking, and enrichment analyses are computational predictions that generated hypotheses for future experimental testing and do not constitute experimental validation.

Nevertheless, the current evidence supports an association between BJSE administration and reproductive improvements rather than confirmation of a specific causal signaling mechanism. Further biochemical and functional investigations are required to determine the contributions of individual constituents, validate predicted molecular interactions, and establish whether the observed changes improve fertility outcomes.

## CONCLUSION

This study showed that BJSE administration improved several semen quality parameters in male rabbits, including sperm survival, motility, acrosome integrity, and morphology. These improvements were generally dose-dependent, with the most pronounced responses observed at 600 mg/kg body weight. BJSE administration also caused time-dependent changes in serum reproductive hormone concentrations and increased testicular expression of mTOR, Akt1, and HSPA2, along with reduced PTEN expression. Chemical profiling identified 29 major constituents, whereas network pharmacology and molecular docking identified potential bioactive compounds and reproductive signaling-related targets.

These findings provide preliminary experimental evidence supporting further investigation of BJSE as a potential herbal preparation to improve semen quality and sperm motility. The observed dose-associated responses may inform subsequent dose optimization studies, while the identified chemical constituents provide a foundation for developing standardized extract preparations. However, the findings are limited to the experimental rabbit model and do not establish clinical efficacy or improved fertility outcomes.

BJSE administration improved sperm quality and motility in rabbits, accompanied by coordinated changes in PTEN, mTOR, Akt1, and HSPA2 expression. These findings identify the PTEN/mTOR/Akt1/HSPA2 signaling-related network as a potential molecular mechanism warranting further investigation. Nevertheless, the available evidence demonstrates associations rather than a confirmed causal pathway. Further functional validation and reproductive outcome studies are required before the therapeutic potential of BJSE for male infertility can be established.

## DATA AVAILABILITY

The raw UPLC-Q-Orbitrap MS spectra, compound identification confidence table, network pharmacology input and output files, molecular docking configuration files, qPCR Cq values and corresponding calculations, uncropped Western blot images, and individual-animal semen and hormone data are provided in the Supplementary Files. The supplementary files are available from the corresponding author.

## GENERATIVE AI DECLARATION

No generative AI or AI-assisted technologies were used in the preparation, writing, translation, or editing of this manuscript. All content is the authors' original work

## AUTHORS' CONTRIBUTIONS

SW and YC: Contributed equally to this work; Conducted the experiments, processed the samples, formal analyses, and curated the data. YY and JZ: Conceptualized the study, administered the project, acquired funding, and contributed to software development and validation. YW, ML, and JW: Formal analyses and figure preparation. SW and YC: Prepared the original manuscript draft. All authors have reviewed and edited the manuscript and approved the final version.

## ACKNOWLEDGMENTS

This study was financially supported by the Youth Sailing Program Project of Guizhou University of Traditional Chinese Medicine (QNYFZK-2024, No. 11) and the Guizhou Province College Students' Innovation and Entrepreneurship Training Program Project (2023, No. 75).

## COMPETING INTERESTS

The authors declare that they have no competing interests.

## PUBLISHER'S NOTE

Veterinary World remains neutral with regard to jurisdictional claims in the published institutional affiliations.

## REFERENCES


1. Agarwal A, Mulgund A, Hamada A, Chyatte MR. A unique view on male infertility around the globe. Reprod Biol Endocrinol. 2015;13:37.
2. Fraga LG, Gismondi JP, Sanvido LV, Lozano AFQ, Teixeira TA, Hallak J. Clinical and laboratory evaluation of male infertility, a detailed practical approach. Arch Med Res. 2024;55(8):103139.
3. Curi SM, Ariagno JI, Chenlo PH, Mendeluk GR, Pugliese MN, Sardi Segovia LM, *et al*. Asthenozoospermia: analysis of a large population. Arch Androl. 2003;49(5):343–349.
4. Wang Y, Xiang M, Zhou Y, Zheng N, Zhang J, Zha X, *et al*. Novel and recurrent hemizygous variants in *BCORL1* cause oligoasthenoteratozoospermia by interfering transcription. Andrology. 2025;13(5):1261–1269.
5. Yu K, Zhang W, Wang Y, Xiang M, Zheng N, Zhang J, *et al*. A missense mutation in *TCFL5* is associated with male infertility due to oligoasthenoteratozoospermia. Mol Genet Genomics. 2025;300(1):72.
6. Schlegel PN. Aromatase inhibitors for male infertility. Fertil Steril. 2012;98(6):1359–1362.
7. Pozzi E, Corsini C, Salonia A. Medical therapy for male infertility. Curr Opin Urol. 2025;35(2):157–164.
8. Çayan S, Altay AB, Rambhatla A, Colpi GM, Agarwal A. Is there a role for hormonal therapy in men with oligoasthenoteratozoospermia (OAT)? J Clin Med. 2024;14(1):185.
9. Yang C, Li P, Li Z. Clinical application of aromatase inhibitors to treat male infertility. Hum Reprod Update. 2021;28(1):30–50.
10. de Ligny W, Smits RM, Mackenzie-Proctor R, Jordan V, Fleischer K, de Bruin JP, *et al*. Antioxidants for male subfertility. Cochrane Database Syst Rev. 2022;5(5):CD007411.
11. Rambhatla A, Shah R, Pinggera GM, Mostafa T, Atmoko W, Saleh R, *et al*. Pharmacological therapies for male infertility. Pharmacol Rev. 2024;PHARMREV-AR-2023-001085.
12. Ali M, Martinez M, Parekh N. Are antioxidants a viable treatment option for male infertility? Andrologia. 2021;53(1):e13644.
13. Wang M, Wang Q, Du Y, Jiang H, Zhang X. Vitamins combined with traditional Chinese medicine for male infertility: a systematic review and meta-analysis. Andrology. 2020;8(5):1038–1050.
14. Chen ZM, Ao MY, Liao YJ, Yu LY, Yang Zh, Hu L, *et al*. Wuzi Yanzong prescription from Traditional Chinese Medicine for male infertility: a narrative review. J Tradit Chin Med. 2023;43(2):416–428.
15. Li Q, Zhang C, Li C, Lin X, Wang M, Wu L, *et al*. The effectiveness and safety of traditional Chinese herbal medicine for the treatment of male infertility associated with sperm DNA fragmentation: a protocol for systematic review and meta-analysis. Medicine. 2021;100(9):e24918.
16. Bai X, Liu Z, Tang T, Yu S, Liu D, Liu G, *et al*. An integrative approach to uncover the components, mechanisms, and functions of traditional Chinese medicine prescriptions on male infertility. Front Pharmacol. 2022;13:794448.
17. Jiang D, Coscione A, Li L, Zeng BY. Effect of Chinese herbal medicine on male infertility. Int Rev Neurobiol. 2017;135:279–311.
18. Ahmadian M, Salari R, Noras MR, Bahrami-Taghanaki HR. Herbal medicines for idiopathic male infertility: a systematic review. Curr Drug Discov Technol. 2022;19(6):e200822207800.
19. Melnikovova I, Russo D, Fait T, Kolarova M, Tauchen J, Kushniruk N, *et al*. Evaluation of the effect of *Lepidium meyenii* Walpers in infertile patients: a randomized, double-blind, placebo-controlled trial. Phytother Res. 2021;35(11):6359–6368.
20. Han Y. Zhonghua yi shi za zhi (Beijing, China: 1980), 2010;40(4): 198–205.
21. Cheng N, Wang H, Hao H, Rahman FU, Zhang Y. Research progress on polysaccharide components of *Cistanche deserticola* as potential pharmaceutical agents. Eur J Med Chem. 2023;245(Pt 1):114892.
22. Li Z, Li J, Li Y, Guo L, Xu P, Du H, *et al*. The role of Cistanches Herba and its ingredients in improving reproductive outcomes: a comprehensive review. Phytomedicine. 2024; 129:155681.

23. Zhang ML, Li WX, Wang XY, Chen XF, Zhang H, Meng GQ, *et al*. Characterizing metabolomic and transcriptomic changes, and investigating the therapeutic mechanism of *Psoralea corylifolia* Linn. in the treatment of kidney-yang deficiency syndrome in rats. Heliyon. 2024;12(21):e39006.
24. Kamali F, Mojani-Qomi MS, Arbabi Bidgoli S, Lavasani Z, Adineh M. Fennel (*Foeniculum vulgare*) oral capsules improve endometrial thickness in infertile women following clomiphene citrate treatment. Eur J Obstet Gynecol Reprod Biol. 2025;313:114638.
25. Zhou M, Li X, Xiao N, Tan Z. One mechanism of Sishen Pill on diarrhea with kidney Yang deficiency syndrome: influencing metabolic function by intestinal microorganisms and enzyme activity mediates the gut-kidney axis. Front Cell Infect Microbiol. 2025;15:1620789.
26. İpçak HH, Denli M, Yokuş B, Bademkıran S. The impact of dietary encapsulated fennel seed (*Foeniculum vulgare* Mill.) essential oil inclusion levels on performance, serum hormone profiles, and expression of reproductive axis-related genes in the early and late laying phases of hens. Vet Med Sci. 2025;11(1):e70150.
27. Li X, Li X, Wang L, Hou Y, Liu Y, Mao J, *et al*. Advancing traditional Chinese medicine research through network pharmacology: strategies for target identification, mechanism elucidation and innovative therapeutic applications. Am J Chin Med. 2025;53(7):2021–2042.
28. Hopkins AL. Network pharmacology: the next paradigm in drug discovery. Nat Chem Biol. 2008;4(11):682–690.
29. Bustani G, Alghetaa H, Mohammed A, Nagarkatti M, Nagarkatti P. The aryl hydrocarbon receptor: a new frontier in male reproductive system. Reprod Biol Endocrinol. 2025;23(1):70.
30. Zhao Z, Qi HY, Li ZF, Wang LM, Wang JM, Tan FQ, *et al*. *Vangl2* regulates intercellular junctions by remodeling actin-based cytoskeleton through the Rock signaling pathway during spermatogenesis in *Eriocheir sinensis*. Int J Biol Macromol. 2024;279:135264.
31. Yu P, Zhao X, Zhou D, Wang S, Hu Z, Lian K, *et al*. The microRNA-mediated apoptotic signaling axis in male reproduction: a possible and targetable culprit in male infertility. Cell Biol Toxicol. 2025;41(1):54.
32. Deng CY, Lv M, Luo BH, Zhao SZ, Mo ZC, Xie YJ. The role of the *PI3K*/*AKT*/*mTOR* signalling pathway in male reproduction. Curr Mol Med. 2021;21(7):539–548.
33. Long C, Zhou Y, Shen L, Yu Y, Hu D, Liu X, *et al*. Retinoic acid can improve autophagy through depression of the *PI3K-Akt-mTOR* signaling pathway via *RARα* to restore spermatogenesis in cryptorchid infertile rats. Genes Dis. 2021;9(5):1368–1377.
34. Dun MD, Smith ND, Baker MA, Lin M, Aitken RJ, Nixon B. The chaperonin containing TCP1 complex (CCT/TRiC) is involved in mediating sperm-oocyte interaction. J Biol Chem. 2011;286(42):36875–36887.
35. Lin HK, Wang L, Hu YC, Altuwaijri S, Chang C. Phosphorylation-dependent ubiquitylation and degradation of androgen receptor by Akt require Mdm2 E3 ligase. EMBO J. 2002;21(15):4037–4048.
36. Heemers HV, Tindall DJ. Androgen receptor (AR) coregulators: a diversity of functions converging on and regulating the AR transcriptional complex. Endocr Rev. 2007;28(7):778–808.
37. Plotnikova OV, Nikonova AS, Loskutov YV, Kozyulina PY, Pugacheva EN, Golemis EA. Calmodulin activation of Aurora-A kinase (*AURKA*) is required during ciliary disassembly and in mitosis. Mol Biol Cell. 2012;23(14):2658–2670.
38. Dumasia K, Kumar A, Deshpande S, Balasinor NH. Estrogen, through estrogen receptor 1, regulates histone modifications and chromatin remodeling during spermatogenesis in adult rats. Epigenetics. 2017;12(11):953–963.
39. Nanjappa MK, Hess RA, Medrano TI, Locker SH, Levin ER, Cooke PS. Membrane-localized estrogen receptor 1 is required for normal male reproductive development and function in mice. Endocrinology. 2016;157(7):2909–2919.
40. Luo H, Huang Y, Han M, Pang Y, Yu P, Tang Y, *et al*. Associations of serum estradiol level, serum estrogen receptor-alpha level, and estrogen receptor-alpha polymorphism with male infertility: a retrospective study. Medicine. 2021;100(29):e26577.
41. Li YC, Luo ML, Guo H, Wang TT, Lin SR, Chen JB, *et al*. Identification of *NR0B1* as a novel androgen receptor co-repressor in mouse Sertoli cells. Int J Mol Med. 2016;38(3):853–860.
42. Simoncini T, Hafezi-Moghadam A, Brazil DP, Ley K, Chin WW, Liao JK. Interaction of oestrogen receptor with the regulatory subunit of phosphatidylinositol-3-OH kinase. Nature. 2000;407(6803):538–541.
43. Xiao X, Ni Y, Yu C, Li L, Mao B, Yang Y, *et al*. Src family kinases (SFKs) and cell polarity in the testis. Semin Cell Dev Biol. 2018;81:46–53.

44. Xiao X, Yang Y, Mao B, Cheng CY, Ni Y. Emerging role for SRC family kinases in junction dynamics during spermatogenesis. Reproduction. 2019;157(3):R85–R94.
45. Nixon B, Bromfield EG, Cui J, De Iuliis GN. Heat shock protein A2 (*HSPA2*): regulatory roles in germ cell development and sperm function. Adv Anat Embryol Cell Biol. 2017;222:67–93.
46. Nixon B, Bromfield EG, Dun MD, Redgrove KA, McLaughlin EA, Aitken RJ. The role of the molecular chaperone heat shock protein A2 (*HSPA2*) in regulating human sperm-egg recognition. Asian J Androl. 2015;17(4):568–573.
47. Szklarczyk D, Gable AL, Nastou KC, Lyon D, Kirsch R, Pyysalo S, *et al*. The STRING database in 2021: customizable protein-protein networks, and functional characterization of user-uploaded gene/measurement sets. Nucleic Acids Res. 2021;49(D1):D605–D612.
48. Ji L, Song T, Ge C, Wu Q, Ma L, Chen X, *et al*. Identification of bioactive compounds and potential mechanisms of scutellariae radix-coptidis rhizoma in the treatment of atherosclerosis by integrating network pharmacology and experimental validation. Biomed Pharmacother. 2023;165:115210.
49. Zhang Y, Sanner MF. AutoDock CrankPep: combining folding and docking to predict protein-peptide complexes. Bioinformatics. 2019;35(24):5121–5127.
50. Eberhardt J, Santos-Martins D, Tillack AF, Forli S. AutoDock Vina 1.2.0: new docking methods, expanded force field, and Python bindings. J Chem Inf Model. 2021;61(8):3891–3898.
51. Barth AD, Arteaga AA, Brito LF, Palmer CW. Use of internal artificial vaginas for breeding soundness evaluation in range bulls: an alternative for electroejaculation allowing observation of sex drive and mating ability. Anim Reprod Sci. 2004;84(3–4):315–325.
52. Hsin KY, Ghosh S, Kitano H. Combining machine learning systems and multiple docking simulation packages to improve docking prediction reliability for network pharmacology. PLoS One. 2013;8(12):e83922.
53. Sabeti P, Amidi F, Kalantar SM, Sedighi Gilani MA, Pourmasumi S, Najafi A, *et al*. Evaluation of intracellular anion superoxide level, heat shock protein A2 and protamine positive spermatozoa percentages in teratoasthenozoospermia. Int J Reprod Biomed. 2017;15(5):279–286.
54. Kowalczyk P, Sulejczak D, Kleczkowska P, Bukowska-Ośko I, Kucia M, Popiel M, *et al*. Mitochondrial oxidative stress—a causative factor and therapeutic target in many diseases. Int J Mol Sci. 2021;22(24):13384.
55. Zhao H, Liu J, Song L, Liu Z, Han G, Yuan D, *et al*. Oleanolic acid rejuvenates testicular function through attenuating germ cell DNA damage and apoptosis via deactivation of *NF-κB*, *p53* and *p38* signalling pathways. J Pharm Pharmacol. 2017;69(3):295–304.
56. Yan L, Wang J, Dai D, Zhang Y, Li Y, Xiao W. Testicular protective effects of hesperidin against chemical and biological toxicants. Toxicol Res. 2024;13(3):tfae078.
57. Abu-Khudir R, Almutairi HH, Abd El-Rahman SS, El-Said KS. The palliative and antioxidant effects of hesperidin against lead-acetate-induced testicular injury in male Wistar rats. Biomedicines. 2023;11(9):2390.
58. Ijaz MU, Tahir A, Ahmed H, Ashraf A, Ahmedah HT, Muntean L, *et al*. Chemoprotective effect of vitexin against cisplatin-induced biochemical, spermatological, steroidogenic, hormonal, apoptotic and histopathological damages in the testes of Sprague-Dawley rats. Saudi Pharm J. 2022;30(5):519–526.
59. Xin S, Xiaoxuan L, Yixuan Z, Zhikang C. Leptin promotes proliferation of human undifferentiated spermatogonia by activating the *PI3K*/*AKT*/*mTOR* pathway. Am J Reprod Immunol. 2024;91(1):e13811.
60. Lahimer M, Capelle S, Lefranc E, Bosquet D, Kazdar N, Ledu A, *et al*. Micronutrient-antioxidant therapy and male fertility improvement during ART cycles. Nutrients. 2025;17(2):324.
61. Lai PF, Mahendran R, Tsai BC, Lu CY, Kuo CH, Lin KH, *et al*. Calycosin enhances heat shock related-proteins in H9c2 cells to modulate survival and apoptosis against heat shock. Am J Chin Med. 2024;52(4):1173–1193.
62. Oduwole OO, Huhtaniemi IT, Misrahi M. The roles of luteinizing hormone, follicle-stimulating hormone and testosterone in spermatogenesis and folliculogenesis revisited. Int J Mol Sci. 2021;22(23):12735.
63. Ghasemi N, Azizi H, Razavi-Amoli SK, Skutella T. The role of Plzf in spermatogonial stem cell maintenance and differentiation: mapping the transcriptional dynamics and key interactions. Cells. 2024;13(23):1930.


********